

AD-A135 651

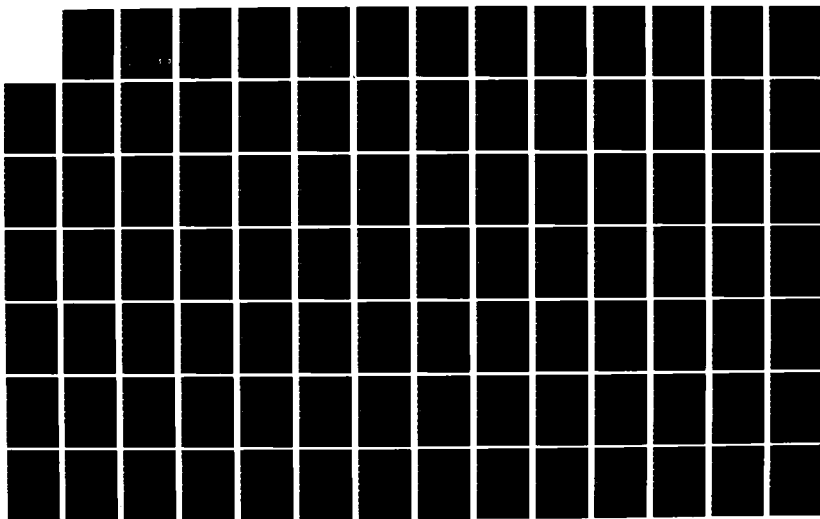
DISCHARGE UNDER THE COMBINED INFLUENCE OF DC AND RF
FIELDS(U) AIR FORCE INST OF TECH WRIGHT-PATTERSON AFB
OH SCHOOL OF ENGINEERING J A THORNE DEC 82
AFIT/GEO/PH/82D-14

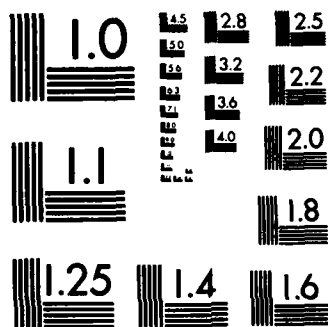
1/2

UNCLASSIFIED

F/G 28/3

NL





MICROCOPY RESOLUTION TEST CHART
NATIONAL BUREAU OF STANDARDS-1963-A

1

AD-A735-652

DISCHARGE UNDER THE COMBINED
INFLUENCE OF DC AND RF FIELDS

THESIS

AFIT/GEO/PH/82D-14

Jeremy A. Thorne
1Lt USAF

DTIC FILE COPY

DTIC
ELECTE
DEC 12 1983

B

Approved for public release; distribution unlimited.

83 12 12 066

DISCHARGE UNDER THE COMBINED
INFLUENCE OF DC AND RF FIELDS

THESIS

Presented to the Faculty of the School of Engineering
of the Air Force Institute of Technology

Air University

In Partial Fulfillment of the
Requirements for the Degree of
Master of Science

by

Jeremy A. Thorne

1 Lt USAF

Graduate Electro-Optics

December 1982

Approved for public release; distribution unlimited.

Preface

This thesis initiated a feasibility study of externally controlled switches using microwave excitation. This work was to complement similar work that is being done with electron beam switches. Since the microwave equipment needed to externally maintain a discharge does not have the complexity of an e-beam machine, this approach may more easily identify optimum parameter ranges that may be used for all switch technology. Initially, a simple experiment was conceived to determine the current-voltage characteristics. From this, the magnitude of the electron drift velocity and its dependence on electric field could be inferred. Interest in the drift velocity has come from the observation of "negative differential conductivity" in certain gas mixtures. More experimental data in this area would help verify the theoretical calculations and possibly point the direction for further switch research.

As the experimental work proceeded, results indicated that the current-voltage curve was influenced by sheath effects. The effort then was redirected toward obtaining data which may provide a better understanding of discharges under these conditions.

I would like to express my appreciation to the AFWAL Energy Conversion Branch for their support in this experiment. I am grateful for the privilege to have been able to work with Dr Alan Garscadden who suggested this project. His presence

and help has been most important during this project. Also, Dr William Bailey was of great assistance in helping me to understand some of the fundamental physics involved in this investigation.

I would also like to acknowledge the day-to-day experimental and theoretical support given by Dr Merrill Andrews of Wright State University, Ohio. It was his insight that provided the foundation and development of Model II in the theory section. With Dr Andrews as mentor, I began to gain a greater understanding and appreciation for the physics involved in electric discharges. Also, at his side, many aspects of mathematics and physics took on greater meaning.

My greatest appreciation goes to my wife, Hiltrud and children, Natasha and Shawn; it was on their support that I relied the most. This has only been possible through their unselfish sharing of their husband and father.

Accession For	
NTIS GRA&I	<input checked="checked" type="checkbox"/>
DTIC TAB	<input type="checkbox"/>
Unannounced	<input type="checkbox"/>
Justification	
By	
Distribution/	
Availability Codes	
Dist	Avail and/or Special
A-1	



Contents

	<u>Page</u>
Preface	ii
List of Figures	vi
List of Symbols	vii
Abstract	x
I. Introduction	1
Background	2
Problem	5
Assumptions	5
Approach	6
Sequence of Presentation	6
II. Theory	7
Kinetic Theory	9
Collisions	11
Cross-section	12
Drift Velocity and Mobility	14
Diffusion	17
Charge Carriers, Production	19
Charge Carriers, Losses	23
Gas Discharge	26
Low Pressure Glow Discharge	31
Model I	34
Model II	37
III. Equipment	51
Microwave Sources	51
Microwave Components-Loads, Circulators, and Detectors	52
Applicator	56
Interlock System	59
Discharge Tubes	61
Gas and Vacuum System	63
DC Source and Diagnostics	65
IV. Procedure and Results	70
Gas/Vacuum System	70
Microwave Power Meter Calibration	71
Power-Up, Power-Down	74

	<u>Page</u>
I-VC For Discharge Tube I	75
I-VC For Discharge Tube II	77
V. Analysis and Conclusions	86
Initial Data, He and He-N	86
DC Characteristics in the Longitudinal	
Tube	89
Pulse Characteristics	93
Conclusions	95
VI. Recommendations	98
Bibliography	100
Appendix: Data Curves for Pulse Measurements . .	102
Vita	112

List of Figures

<u>Figure</u>		<u>Page</u>
1	Drift Velocity for Argon-Nitrogen Mixtures	16
2	Discharge Current-Voltage Curve	28
3	Regions of a Glow Discharge	32
4	Analytic Model of an Externally Sustained Discharge	40
5	Model II Sign Conventions	45
6	Experimental Arrangement	53
7	Microwave Applicator	57
8	Applicator Fields with a Discharge Tube	60
9	Discharge Tubes	62
10	Gas and Vacuum System	64
11	System Leak-up	64
12	Diagnostics for Discharge Tube I	66
13	DC Diagnostics for Discharge Tube II	66
14	Diagnostics for Pulsed Measurements	69
15	Power Meter Calibration	73
16	I-V Characteristics for 10% N-He in Tube I	78
17	I-V Characteristics for 100% He in Tube II	79
18	DC Characteristics for Tube II	81
19-27	Pulsed I-V Characteristics for Discharge Tube II	103-111

List of Symbols

A	Area
b	Cathode sheath thickness
C	Coulomb
cm	Centimeter
D	Diffusion coefficient (cm^2/sec)
D_a	Ambipolar diffusion coefficient (cm^2/sec)
D_e	Diffusion coefficient for electrons (cm^2/sec)
D_L	Longitudinal diffusional coefficient for electrons (cm^2/sec)
D_+	Diffusion coefficient for ions (cm^2/sec)
E	Electric field strength (V/cm)
E_e	Effective electric field strength (V/cm)
e	Electronic charge (1.6×10^{-19} Coulombs)
eV	Electron volt
ϵ	Energy
h_i	Ionization efficiency
h_x	Excitation efficiency
I	Current (amperes)
j	Flux density ($1/\text{cm}^2/\text{sec}$)
j_e	Electron flux density ($1/\text{cm}^2/\text{sec}$)
j_+	Positive ion flux density ($1/\text{cm}^2/\text{sec}$)
k	Boltzmann's constant (1.38×10^{-23} Joules/ $^{\circ}\text{K}$)
KV	Kilovolt (1000 volts)
L	Electrode spacing (cm)
l	Mean free path (cm)

l_d	Mean free path for momentum transfer (cm)
m	Mass
mA	Milliampere (.001 ampere)
N	Neutral number density ($1/\text{cm}^3$)
n	Number of moles
n_e	Electron number density ($1/\text{cm}^3$)
n_i	Ion number density (usually positive) ($1/\text{cm}^3$)
n_+	Positive ion density ($1/\text{cm}^3$)
n_{eo}	Electron density in the positive column ($1/\text{cm}^3$)
n_{+o}	Positive ion density in the positive column ($1/\text{cm}^3$)
P, p	Pressure
P_c	Probability for collision ($\text{cm}^2/\text{cm}^3/\text{torr}$)
P_i	Probability for ionization ($\text{cm}^2/\text{cm}^3/\text{torr}$)
P_x	Probability for excitation ($\text{cm}^2/\text{cm}^3/\text{torr}$)
Q_c	Cross-section for collision (\AA^2)
Q_d	Cross-section for momentum transfer (\AA^2)
R	Universal gas constant (8314 J/kmole/ $^\circ\text{K}$)
R	Recombination rate coefficient (cm^3/sec)
R	Resistance (volts/ampere)
S	Electron-ion pair production rate ($1/\text{cm}^3/\text{sec}$)
t	Time (sec)
T	Temperature (degrees Kelvin)
T_d	Townsend ($1 \times 10^{-17} \text{ V-cm}^2$)
T_e	Average temperature of the electrons (eV)
T_i	Average temperature of the ions (eV)
U_i	Ionization energy (eV)

V	Volume (cm^3)
V	Volt
V_c	Voltage drop across the cathode sheath (volts)
v	Velocity (cm/sec)
v_a	Ambipolar velocity (cm/sec)
v_d	Diffusion velocity (cm/sec)
W	Drift velocity (cm/sec)
W_e	Electron drift velocity (cm/sec)
W_i	Ion drift velocity (cm/sec)
x	Distance (cm)
α	Townsend ionization coefficient ($1/\text{cm}$)
γ	Secondary emission coefficient (electron/incident ion)
ϵ	Permittivity of free space ($8.85 \times 10^{-14} \text{C/volt/cm}$)
η	Ionization coefficient (ion-electron pair/volt)
Λ	Diffusion length (cm)
Λ_a	Transverse diffusion length (cm)
Λ_L	Longitudinal diffusional length (cm)
μ	Mobility ($\text{cm}^2/\text{volt/sec}$)
μ_e	Electron mobility ($\text{cm}^2/\text{volt/sec}$)
ν_c	Collision frequency ($1/\text{sec}$)
ν_m	Collision frequency for momentum transfer ($1/\text{sec}$)
ν_i	Ionization frequency ($1/\text{sec}$)
σ	Conductivity (ampere/volt/cm)
τ_d	Diffusion time (sec)
τ_m	Time between collisions for momentum transfer (sec)
ω	Angular frequency ($1/\text{sec}$)

Abstract

Cold cathode discharges in argon and argon-nitrogen mixtures were investigated experimentally. Current-voltage characteristics were obtained experimentally for these in microwave sustained discharges. The current-voltage characteristics show current saturating at low values of E/N followed by a rapid increase in current at higher E/N . Lowke's theoretical investigation¹ of gas discharges sustained by an external ionizing source was extended to include microwave excitation. This analysis predicted similar saturation for the current in the current-voltage characteristics.

¹ J. J. Lowke, D. K. Davies, J. Appl. Phys. 48(12): 4991 (1977).

DISCHARGE UNDER THE COMBINED INFLUENCE OF DC AND RF FIELDS

I. Introduction

At the heart of the development of high energy physics, including lasers and particle beam weapons, is the source of power. What research demands now is megajoules of energy on a microsecond time scale. The most critical component in pulse power systems which will be able to supply this power is the switch. Of particular importance are switches which are not limited to single shot or low repetition rate operation. Switching for repetitive operation is considered to be one element that is pacing particle beam and shorter wavelength weapon technology (Ref 1:70). In the past, energy storage devices for pulse power have been capacitors. The energy storage density of inductive systems may exceed that of capacitive systems by an order of magnitude or more. With capacitive energy storage, spark gap switches are commonly used to control the power application to the load. Inductive systems require switches that will open as well as close. This can not be accomplished with a spark gap. Opening circuits, in which current drops quickly to zero, have high values of di/dt . With the voltage developed across a switch $V = L di/dt$, inductive storage (L) and fast switch off create switch voltages that are easily beyond the stand off or insulating voltage. A key technological problem in developing an inductive

energy storage system, then, is the opening switch. The spark gap is not capable of "switch off" and is difficult to operate in a repetitive mode.

Background

To gain on/off control and repetitive operation, researchers are looking at externally sustained discharges. When the external source of ionization is removed, the discharge will extinguish and current will stop. Lasers, electron beams and radio frequency sources are all under consideration to control the switching discharge (Ref 2).

A computer model (Ref 3), developed by Westinghouse Electric Corporation for the Aero Propulsion Laboratory, compares the performance parameters for high voltage on/off switches. Their model was patterned after work done in modeling high power lasers and used an electron beam to sustain the discharge. Their results indicate that performance of the electron beam switch will be strongly dependent upon the discharge gas properties. These include high dielectric strength, high values of electron drift velocity, high secondary electron production rate by the control beam electrons, and low recombination rate coefficients (Ref 3).

With electron beam ionization as a source of conduction electrons, the discharge becomes a volume conductor spreading the current flow out over many square centimeters. The efficiency of the e-beam switch depends on the current gain or ratio of current switched to beam current. Bletzinger (Ref 4)

has been able to demonstrate current gains of as high as 1000 in methane. Adding argon to the methane improved the conductivity and current gain.

Others have looked at the non-self sustained discharge (Refs 5, 6, 7, 8). Ward (Ref 5:1852) has shown the effect of a variation in the initial photocurrent density on the static characteristics of argon back in 1958. Averin (Ref 6:665), in his theoretical description of the current voltage characteristics of a non self-sustained volume discharge, draws attention to regions of negative differential conductivity. Zakharov (Ref 7:1074) studied the temporal evolution of an externally ionized discharge. The region near the cathode is examined and Zakharov also sees negative differential conductivity. Lowke and Davies (Ref 8:4991) theoretically examined externally maintained discharges of the kinds that would be found in gamma ray photoionization and fission fragment ionization chambers and the electron beam laser. Hallada (Ref 9) later extended their work to include effects of other discharge electron generation and loss processes.

As opposed to considering applications solely for switch operation, much of the work on externally sustained discharges has, like those mentioned, used nuclear or ionizing radiation as would be found in radiation detectors and counters, or in the area of electron beam discharges that may be applied to laser technology. The simultaneous use of high frequency electric fields to sustain a discharge while examining the DC

characteristics has been considered by Yamamoto and Okuda (Ref 10:144). They looked at discharges ranging from a DC glow to the space charge limited case in which the DC and AC fields were perpendicular. Lobov and Zakharov (Ref 11:614) have investigated the effect of a microwave field on the electron drift velocity. They found that the addition of microwave power resulted in an increase in the directional electron velocity with a consequent rise in discharge current. They also show that the total electron energy increases in the presence of the microwave field and that the energy distribution function becomes broader, its peak decreases and moves out to higher energies.

The use of mixtures of gases that have significantly different properties than its components such as neon-argon Penning mixtures is not new. Also, the use of electronegative gases in switches is a standard practice to increase their insulating properties. Of new interest is the change in the electron drift velocity with change in electric field and its possible application in switch technology. In Ramsauer gases (argon, krypton, and xenon), which have a minimum in their momentum transfer cross-section, the addition of a molecular gas can dramatically influence the electron drift velocity. In a discharge, this results in a negative differential conductivity over a certain range of E/N which may have an important impact on the optimization of switch gas mixtures, particularly in terms of ON/OFF operations.

Nagy (Ref 12:327) found that even a small amount (0.1%) of nitrogen in argon has considerable effect on the value of drift velocity. Experiments to measure electron drift velocity in argon have often given strange or misleading results. It is now recognized that this was probably due to impurities. Long (Ref 13:471) has developed an analytical approximation with gas type related constants that relate the drift velocity to the amount and type of molecular gas in argon and helium.

Problem

The objective of this experiment was to obtain current-voltage characteristic curves for a microwave excited discharge. The discharges examined were to use various gases including pure argon, helium, and specified percentages of nitrogen mixed in argon.

Assumptions

The major assumptions are more fully developed in the theory section. First, the microwave discharge was assumed to be a uniform plasma between the electrodes. Second, it was assumed that there would be no sheath effects that would alter the uniformity of the electric field between the electrodes. Third, for the results to give reasonable information as to the magnitude of the drift velocity, it was assumed that the electron mean free path was much shorter than the electrode separation. Fourth, the ionization rate or electron production due to the microwaves was assumed to be much greater than the rate of loss due to conduction.

Approach

The basic procedure used to generate the current-voltage characteristics (I-VC) was to vary the voltage across the microwave discharge while monitoring the subsequent current. This began by using a function generator and voltage amplifier as the voltage source. After the discharge tube was changed to one with larger electrode separation, the voltage source used was a high voltage power supply that was manually adjusted. In both cases the I-VC were plotted on an X-Y recorder. Final I-VC curves were obtained using pulse voltage application and using an oscilloscope to determine the voltage and discharge current magnitudes.

Sequence of Presentation

First, a theory section will be presented which will contain a general background discussion of important discharge characteristics including kinetic theory, production and loss of charge carriers in a discharge, types of discharges, structure of a low pressure discharge, and two models which are the basis for the analysis. Next, there will be a description of the experimental setup and the equipment that was used. Third, the procedures used to obtain the data will be presented along with the results of the measurements. Fourth, the data will be analyzed in view of the theory developed in that section. Finally, conclusions about the results and recommendations will be presented.

II. Theory

The capability of a switch to open quickly is important for inductive energy storage systems. At the same time switching current off in an inductive circuit is made more difficult by the inductance, because the induced voltage tends to keep the current flowing. Since switch control for an externally ionized switch plasma should depend only on the source, it would be undesirable for the switch to go into an avalanche mode. The continuity equation for the electrons which contribute to conduction is

$$\frac{dn_e}{dt} = S + n_e \alpha |W| + [\text{Loss Terms}] \quad (1)$$

There is a similar equation for ions. In this equation S is the source function which is to control the switch. The $n_e \alpha |W|$ term is an ionizing term that produces electron-ion pairs, where n_e is the electron density, α is Townsend's first ionization coefficient, and W is the electron drift velocity. The loss terms include diffusion, recombination, and attachment.

Switch off takes place when the source term S is removed, providing the other production terms do not exceed the loss terms. Under certain conditions, the $n_e \alpha |W|$ term can increase rapidly causing a rapid generation of electron-ion pairs and the switch can go into the arc mode of discharge. The drift velocity, W , is dependent on the electric field. At "switch off" a rapid decrease in current (to near zero) is desired;

this means a large di/dt . Since the voltage across an inductor is $L di/dt$, this can place very high voltages across the switch, and if W increases with electric field this may work against switch off.

An ideal switch would exhibit a high conductivity in the conduction stage (high drift velocity with low E/N). During the opening stage, on the other hand, the conductivity should decrease (low drift velocity with high E/N). This behavior is called negative differential conductivity when the conductivity decreases with an increase in E/N . Complementing this ideal behavior of the drift velocity would be an attachment rate which would be low in the on stage and high in the opening stage (Ref 14). These properties are based on the interaction of the charge carriers and the neutral particles in the conducting medium. The collisional processes and the cross-section for these processes will be outlined in this chapter.

The material presented in this chapter will begin with a review of some basic plasma relations in the kinetic theory section. Included in this section are collisions, cross-section, drift velocity and mobility, and diffusion. The next section will describe the production and loss of charge carriers. Carrier production by Townsend ionization will be presented for both DC and AC discharges. Losses include diffusion, recombination, and attachment. Following this will be a general section on gas discharges which will describe a typical current-voltage characteristic curve. In addition,

there will be a comparison of self and externally sustained discharges while describing microwave and electron beam excitation. The next section will describe the structure of a low pressure glow discharge. The division of the discharge into component regions will be presented along with a description of the processes within these regions.

Finally, two models will be presented which are the basis for the experiment. Model I will describe the basic experimental assumptions in some detail. Model II gives an account of the results when cathode sheath effects are present. These models will be considered in light of the experimental results.

Kinetic Theory

Switching in an electrical circuit is usually accomplished through mechanical contacts or a conductive gas discharge. Current flow through a gas medium is accomplished by the movement of charged particles (ions and electrons). Kinetic theory is used to describe the behavior of the particles in the gas that are responsible for transferring charge from one electrode to another in a discharge (current flow). Kinetic theory makes it possible to relate the overall properties of a gas to the average behavior of the particles.

In order to determine the number densities of the atoms or molecules in a gas, the ideal gas law and Avagadro's hypothesis are used. The ideal gas law gives the relationship between pressure, volume, and absolute temperature for a perfect gas.

$$PV = nRT \quad (2)$$

where P is the pressure, V is the volume, R is the universal gas constant, T is the absolute temperature, and n is the number of kilomoles. Avogadro's hypothesis says that under the same conditions of temperature and pressure all gases have the same number of molecules per unit volume. This number is 6.023×10^{23} molecules per mole.

Boltzmann's equation shows the average steady state concentration of ions at different points in an electrostatic field in relation to the potential difference of those points.

$$\frac{n_{+1}}{n_{+2}} = \exp \left[-\frac{e(V_1 - V_2)}{kT} \right] \quad (3)$$

where n_{+1} and n_{+2} are the ion concentrations, e is the electronic charge, V_1 and V_2 are the potentials at points one and two respectively, k is Boltzmann's constant (1.38×10^{-23} joules/ $^{\circ}\text{K}$), and T is the temperature in degrees kelvin. kT and $e(V_1 - V_2)$ have the dimensions of energy. This relationship can be applied to an electron cloud if the electron could behave like a perfect gas.

The steady state motion of the molecules (atoms) in a gas is divided evenly between coordinate directions X, Y, and Z. The velocities of the particles, however, are distributed through a broad range of velocities. The equilibrium distribution of the velocities of these particles takes the form of

a Maxwellian Distribution. The RMS velocity of this distribution of particles is $\sqrt{3kT/m}$, from this the mean particle energy ($mv^2/2$) is $3kT/2$. The energy then is directly proportional to the atom temperature. The electrons and ions in a plasma also have a thermal energy distribution.

Collisions

Collisions occur as a result of the random thermal motion of the particles. In an electric discharge, in addition to the random thermal motion, a directed velocity component arises due to the application of an electric field. On the average, charged particles will gain energy from the electric field which will be proportional to the strength of the electric field, the time between collisions, and inversely proportional to the mass of the particle. In the steady state, under the influence of the electric field, the average kinetic energy is constant and so is the directed velocity due to the electric field. This directed velocity is called "drift velocity". Though there is a constant force on the particles due to the electric field, the collisions tend to limit or fix the maximum velocity a particle will attain. This is analogous to the macroscopic effect of viscous friction, which here determines the resistivity of the ionized gas (Ref 17:34).

The distance, on the average, that an electron will travel between collisions, can be estimated by the relation $\ell = 1/\pi n R^2$, where ℓ is the mean free path, n is the atom (ion or molecule) density, and R is the radius of the atom. It turns out that calculations of the mean free path from this

relation based on the "elastic sphere of fixed diameter assumption", do not give reasonable values in practice. This relation does show that the mean free path varies inversely with the number density.

The mean free path depends on the electron's cross-section for collision. This collision cross-section depends on the electron velocity (energy). An explanation of this dependency is provided by quantum mechanics. In some gases, electrons show a marked decrease in cross-section at low velocity. This minimum is known as the Ramsauer minimum and gases which exhibit this property are called Ramsauer gases.

Cross-Section

A monoenergetic beam of electrons is passed through a gas with a known number density. Attenuation of the electron beam goes like $I = I_0 \exp(-x/\ell)$, where x is the distance travelled in the gas and ℓ is defined as the mean free path. The cross-section for collision is then

$$Q_c = \frac{1}{\ell N} = 1.034 \times 10^{-19} \left(\frac{1}{\ell} \right) \left(\frac{T}{P} \right) \quad (4)$$

where

$$N = 2.687 \times 10^{19} \left(\frac{P}{760} \right) \left(\frac{273}{T} \right) \text{ cm}^{-3} \quad (5)$$

is the number density, T is the temperature ($^{\circ}\text{K}$), and P is the pressure (torr).

In an elastic collision between the electron and atom, the electron is scattered by the atom. The energy transferred to

the atom by the electron is proportional to the scattering angle and by the change in momentum suffered by the electron. Associated with this process is a momentum transfer cross-section and similarly $Q_d = 1/\ell_d n$, where Q_d is the cross-section for momentum transfer and ℓ is the mean free path for momentum transfer.

Collision probability P_c ($\text{cm}^2/\text{cm}^3/\text{torr}$) is sometimes used to express the electron-atom interactions by setting $\ell P_c p = 1$, where p is the pressure of the gas. Collision probability is then

$$P_c = \frac{1}{p \ell} \quad (6)$$

or collision cross-section in area per cubic centimeter at one torr and 0°C .

$$Q_c = 2.82 \times 10^{-17} P_c \quad (7)$$

with mean free path in centimeters and pressure in torr.

Collision frequency ν_c is the number of collisions per second, on the average, that an electron makes with the gas atoms. If v is the electron speed, then $\nu_c = v/\ell$. Some useful numerical relationships among these quantities are:

$$\nu_c = v P_c = 5.93 \times 10^7 v^{1/2} P_c = 21.0 \times 10^7 v^{1/2} p Q_c \quad (8)$$

(Ref 15:25)

where v is in electron volts, p is in torr, and Q_c is in angstroms squared.

An inelastic collision occurs when an electron collides with an atom (molecule) and some of the electron's kinetic energy is transformed into the internal energy of the atom (molecule). This energy goes into a change in the energy configuration of the atom (vibrational, rotational, or electronic for the molecule). The excited particle may return to its ground state quickly, radiating energy, or remain in an excited state for many milliseconds before radiating its energy. If the incident electron has sufficient energy to ionize the atom, an electron may be removed from the atom. In this case there are two free electrons and a positive ion, the original electron and the electron-ion pair formed by the collision. Efficiency for ionization (h_i) and excitation (h_x) can be expressed as ratios of the probabilities for these processes to the probability for collision, $h_i = P_i/P_c$, $h_x = P_x/P_c$. These efficiencies are a function of the electron energy.

Drift Velocity and Mobility

The drift velocity is usually a function of the electric field strength. For low field strengths (and certain gas conditions) this relation takes the form

$$W = \mu E \quad (9)$$

where μ is the mobility (μ_e for electrons and μ_i for ions).

Electron drift velocity measurements in argon have shown inconsistencies which had been attributed to impurities. In order to account for the drift velocity variation in a molecular gas mixed in with a rare gas, Long, Bailey, and

Garscadden (Ref 13:474) have developed an analytic approximation with an empirical fit for drift velocity

$$W = \frac{E/N}{C_1 X^a + C_2 \exp(-B/X)} \quad (10)$$

where

$$\begin{aligned} C_1 &= C_{11} \rho + C_{12} (1-\rho) & X &= (E/N) \rho^{1/2} \\ C_2 &= C_{21} \rho + C_{22} (1-\rho) & B &= B_1 \rho + B_2 (1-\rho) \end{aligned}$$

values for the constants are gas mixture dependent. Values of W for argon-nitrogen mixtures as calculated by Garscadden (Ref 16) are plotted in Figure 1.

In the case where the drift velocity of the ions is small compared to the average velocity (small electric fields), and assuming that the ions are the same temperature as the gas, and the average electric field directed velocity after collision is zero, then

$$\mu_i \approx \frac{e l}{m \bar{v}} \quad (11)$$

where m is the mass of the ion, and e is the ion charge assuming a single ionization.

This is a simplified equation for the mobility coefficient and is not very accurate, but it does show the dependence on mean free path (direct) and on thermal velocity (proportional to $T^{1/2}$).

The electron mobility, μ_e can be expressed

$$\mu_e = \frac{e}{m} \tau_m = \frac{e}{m} \frac{1}{\nu_m} \quad (12)$$

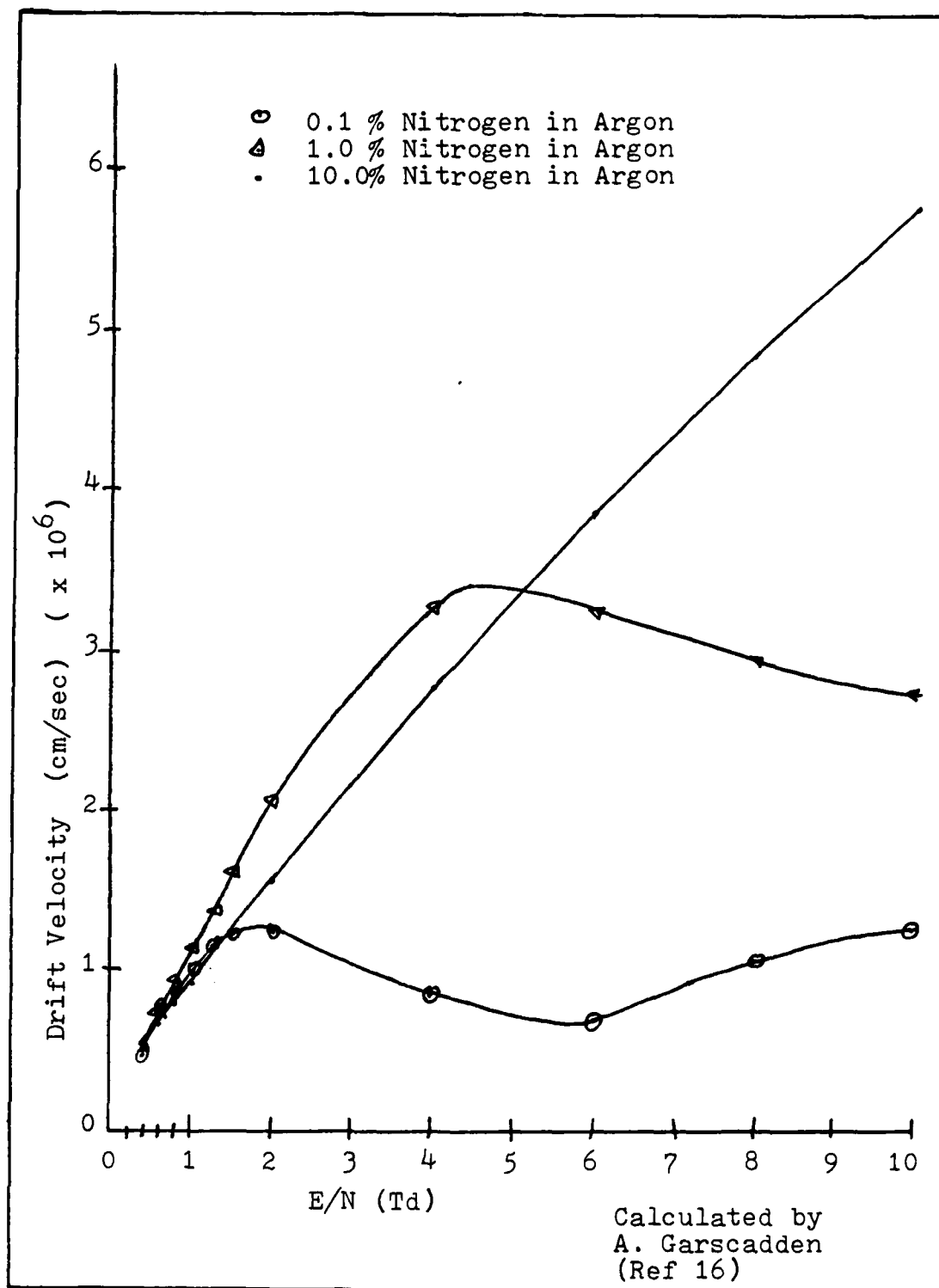


Figure 1. Drift Velocity for Argon-Nitrogen Mixtures

where τ_m is the average time between collisions and ν_m is the collision frequency, $1/\tau_m$. These are based on the collision rate for momentum transfer. Exact values of ν_m may not come directly from the temperature and pressure of the gas and require more detailed knowledge of the distribution of electron energies and the collision cross-section for momentum transfer (Ref 17:35). Exact values for μ_e and μ_i can only be approximated analytically and are more easily obtained from experimental data (Ref 18).

The conductivity or resistivity of an ionized gas can be found from the ion and electron mobilities. Flux density, current density without the charge, in a gas where $n_e = n_+$ (n_+ is singly ionized positive ions) is

$$j_{\text{TOTAL}} = j_+ - j_e = n_e (W_+ - W_e) \quad (13)$$

Because current contributions are made by both electrons and ions this becomes

$$j_{\text{TOTAL}} = n_e E (\mu_i + \mu_e) \quad (14)$$

and conductivity is

$$\sigma = \frac{ej}{E} = n_e e (\mu_i + \mu_e) \approx n_e e \mu_e \quad (15)$$

where $\mu_e \gg \mu_i$, which is often the case.

Diffusion

Diffusion is the movement of charged or uncharged particles from a region of high concentration to one of lower

concentration. The velocity of diffusion is

$$\vec{v}_d = -\frac{D}{N} \nabla N \quad (16)$$

or, in one dimension

$$v_{dx} = -\frac{D}{N} \frac{dN}{dx} \quad (17)$$

Diffusion is due to the thermal motions of the particles in which there is an imbalance in the collisional forces in one direction. The diffusion constants for positive ions, negative ions, and electrons are different. This is due to their differences in mass, clustering of some molecules or atoms around the ions, and the effective cross-section and mean free path for momentum transfer.

For positive ions the ratio of diffusion to mobility is

$$\frac{D_+}{\mu_i} = \frac{kT}{e} \quad (18)$$

A similar relation for electrons

$$\frac{D_e}{\mu_e} = \frac{kT}{e} \quad (19)$$

is weak and yields poor results. A better approximation is

$$D_e = \frac{\bar{v} l}{3} \quad (20)$$

where \bar{v} is the mean velocity of the electrons, which can be many orders of magnitude higher than that for ions, and l is the mean free path for the electrons, which is a function of the drift velocity (Ref 19:141).

In the presence of an electric field, a gas, which contains an appreciable density of electrons and positive ions, produce electric fields due to the relative difference in the rates of diffusion for the electrons and ions. Because the electrons move faster than the ions, the resulting charge separation creates an electric field that tends to retard the electrons and accelerate the ions in the externally applied field. A steady state is reached in which the electrons and ions diffuse at the same velocity. This is called ambipolar diffusion and the ambipolar velocity is

$$v_a = -D_a \frac{1}{n} \frac{dn}{dx} \quad (21)$$

where D_a is the ambipolar diffusion coefficient which is equal to

$$D_a = \frac{D_e \mu_i + D_i \mu_e}{\mu_e} \quad (22)$$

where $\mu_e \gg \mu_i$. This includes the effects of the diffusion rates for both ions and electrons and is greater than either of them alone. If all particles are the same temperature then $D_e \mu_i = D_i \mu_e$ and $D_a = 2D_i = 2kT_e \mu_i / e$. If $T_e \gg T_i$, then $D_e / \mu_e \gg D_i / \mu_i$ or $D_e \mu_i \gg D_i \mu_e$ and then $D_a = D_e \mu_i / \mu_e = kT_e \mu_i / e$ (Ref 19:144).

Charge Carriers, Production

In an ionization chamber, the incident ionizing radiation is measured by measuring the number of electron-ion pairs generated in terms of the current due to a voltage sweeping out these charge carriers. As the voltage across such a

chamber is increased, a point is reached where an increase in the voltage produces no additional current, this is saturation. This occurs when, excluding losses, all the electron-ion pairs are swept out to form current in the external circuit. If the voltage is further increased, there is a rise in the current due to electron-neutral impact ionization.

If there is an increase of d_n electrons in a distance dx , the production rate can be written as $dn = \alpha n_e dx$, where n_e is the number density of electrons, and α is the production rate. Integrating, it becomes $n_e = n_{e0} \exp(\alpha x)$ which corresponds to the observed current variation $I = I_0 \exp(\alpha d)$, when it is integrated over $0 < x < d$, the separation of the electrodes. The term α is called Townsend's first ionization coefficient and its value depends on the electric field strength, pressure, and the gas. α is often expressed in the form α/p and data of α/p as a function of E/p have been measured for many gases. The use of α/p allows for scaling by E/p (or E/N) to other discharge geometries and pressures according to the similarity rule (Ref 19:288). This is so that the number of ionizations is considered against a mean free path and is then a function of the energy the electron gains from the field before the collision.

An equation for α/p has the form

$$\frac{\alpha}{p} = A \exp \left[- \frac{B}{(E/p)} \right] \quad (23)$$

(Ref 19:180)

where A and B are found in tables. The drawback is that there is a limited range of E/p (differing with gas type) over which this relation holds. The actual values of alpha are dependent on more subtle gas parameters such as the electron energy distribution and frequency of ionization upon collision v_i (Ref 20:99).

The ionization coefficient η is related to alpha by $\eta = \alpha/E$, where η is then the number of ion pairs per volt. Experimental values of η for certain mixed gases show a peak due to the interaction of metastables or long lived excited particles. If these metastables have energies at or above the ionization of the background gas, this energy may be transferred, resulting in ionization of the background gas. This is called Penning ionization and is the case with a small percentage of neon in argon.

As ions are accelerated in an electric field some of them gain enough energy to produce secondary electrons at the cathode by ion-cathode bombardment. Gamma (γ), Townsend's second ionization coefficient, is the cathode yield in electrons per incident ion. Effects due to positive ion bombardment of the cathode are not considered here.

In a discharge maintained by a DC electric field, the production of electron-ion pairs (ionization) must exceed the loss due to current flow in the external circuit. If an alternating (AC) field is applied to a discharge tube, the breakdown characteristics are the same as for the DC providing the frequency is very low ($< 1\text{KHz}$) so that the AC period is

much longer than the ion transit time (Ref 17:72). At higher frequencies, however, ionization is different.

DC discharges have two sources of electrons, collisional ionization and secondary emission effects at the electrodes. AC discharges depend only on collisional ionization for electron generation. Background electrons are accelerated by the AC electric field until the average kinetic energy of the electrons is great enough to overcome energy loss in inelastic collisions and diffusion. The energy the electrons gain is a function of E/p . As the pressure increases the mean free path (ℓ) decreases and the increase in energy $\Delta\epsilon$ decreases

$$\mathcal{E} = eV = e \int \bar{\mathbf{E}} \cdot d\bar{\mathbf{l}} \quad (24)$$

In a low frequency field where the angular frequency of the electric field is small compared to the collisional frequency, the electron motion is almost identical to that in a DC field. As the frequency is increased or the pressure is decreased (ω/p increases), collisions no longer occur frequently enough to keep electron drift current in phase with the electric field, and the transfer of energy from the electric field becomes less efficient. At still higher values of ω/p , the electrons oscillate out of phase with the electric field and very little average energy is transferred.

The efficiency of energy transfer from an AC field is expressed as an effective electric field, E_e

$$E_e^2 = E^2 \left[\frac{\nu^2}{\nu^2 + \omega^2} \right] \quad (25)$$

(Ref 21:2)

where ν is the collision frequency ($\nu = v/\ell$) and ω is the frequency of the AC field.

A steady state discharge sustained by an AC electric field occurs when the electron production rate is equal to the loss rate. In the case where the mean free path is small compared to the discharge tube dimensions and the AC frequency is greater than the collision frequency, diffusion theory holds and the ionization rate must be equal to the diffusion rate (attachment and recombination neglected) (Ref 17:73).

Charge Carriers, Losses

Charge carriers near the walls of the discharge tube collide with it and are neutralized. At the walls of the tube the charge density is lower than at the middle. This imbalance in the charge density (gradient) drives the charge toward the walls. The electrons are more mobile and diffuse more rapidly than the ions. The rate of diffusion is the ambipolar diffusion rate, D_a . Also, since cylindrical geometry applies here with the density maximum at the center (axial) and zero at the walls, the density profile is given by the Bessel function of zero order. This goes through zero at 2.405. When the tube radius (0.85cm) is scaled by this, Λ becomes 0.353cm. From von Engel (Ref 19:145), the ambipolar diffusion coefficient D_a is about $3 \times 10^3 \text{ cm}^2/\text{sec}$ at a pressure of 2 millitorr.

The radial diffusion rate is

$$\frac{dn}{dt} = -\frac{D_a}{A^2} n \quad (26)$$

Integrating,

$$n = n_0 e^{-(D_a/A^2)t} \quad (27)$$

The time for the number density to decrease by $1/e$ is the diffusion time τ_a which becomes

$$\tau_a = \frac{A^2}{D_a} = \frac{(.353 \text{ cm})^2}{8 \times 10^3 \text{ cm}^2/\text{sec}} \left(\frac{\rho}{\rho_0}\right) \quad (28)$$

where $D_a = D_{a0}(p/p_0)$ is used to scale the diffusion coefficient.

Another process by which electrons and ions (charge carriers) are removed from the plasma is by recombination. Recombination is a collisional process, that is ions of unlike charge or electrons and positive ions must come close enough to interact. The rate of carrier loss due to recombination depends on the number densities of both species and the probability that a collision will result in recombination. This can be expressed as

$$\frac{dn_e}{dt} = R n_e n_+ \quad (29)$$

where n_e is the electron number density, n_+ is the positive ion concentration, and R is the recombination coefficient.

In a plasma by definition $n_e = n_+$, therefore

$$\frac{dne}{dt} = Rne^2 \quad (30)$$

The probability of recombination depends on the relative speed, decreasing as their relative speed increases. Also, since recombination is dependent on collisions, this process increases with pressure (collision frequency is proportional to pressure). At the lower pressures (about 1 torr) recombination rates are relatively low. For argon, in the range of 15 to 30 torr, R is about 3×10^{-7} (Ref 19:163) and goes with the square root of pressure. This may become a significant process if the plasma density is high, since the rate goes as the square of the electron number density.

When the electronic structure of an atom nearly fills the outer shell, the atom has an affinity for electrons. This electro-negativity exhibited by these atoms (molecules) allows them to become negatively charged by taking on an electron. This process is called attachment. Changing a neutral atom to a negative ion has the effect of removing free mobile electrons from the plasma but does not change the charge balance in the plasma.

Attaching gases are frequently used in switches and high voltage equipment to increase the stand off potential. The breakdown potential is increased when free electrons are removed from the un-ionized gas, this reduces the chances for Townsend breakdown. Attaching gases frequently used are oxygen, carbon monoxide, and sulfur hexafluoride.

The attachment process is a collisional one. The associated cross-section for attachment is much smaller than for most inelastic collisions. Although the process of attachment is important in microwave ionization and pulse power switch operation, it will not be considered due to the types of gases used in this experiment.

Gas Discharge

In order to form a conductive path through a gas there must be free charge carriers to carry the current. An electrically neutral gas would not conduct. There are, however, a number of free electrons and ions (10 - $100/\text{cm}^3$) in any gas as a result of cosmic rays and natural radioactivity. Even under these conditions the amount of current that could flow is immeasurable.

$$I = \frac{e}{(1.6 \times 10^{-19})} \frac{ne}{(10^2)} \frac{W}{(10^6)} \frac{A}{(10^2)} \approx 10^{-11} \text{ amperes} \quad (31)$$

For measurable currents to flow, the electron density (assuming current flow is by electrons alone) must be substantially higher. Some of the mechanisms for producing larger electron densities have been discussed before. The source of these electrons will determine whether a discharge is self-sustained, not self-sustained, or if it is externally sustained.

A non self-sustaining discharge is one in which the charge carriers are thermally generated, the result of cosmic radiation, natural radioactivity, or other external source.

As the voltage across this discharge is increased, more and more of the generated carriers would be swept out (current) until they are drawn out as fast as they are generated. Beyond this point, an increase in voltage does not give a corresponding increase in current. On the current-voltage characteristic curve in Figure 2, the non self-sustaining discharge is represented by the region from 0 volts to the saturation plateau (dark discharge).

As the applied voltage is increased further, the background electrons which were responsible for the current in the non self-sustaining discharge are accelerated through high voltages. If the energy gained by these electrons within one mean free path is greater than the ionization energy for the neutral particles in the gas, ionization will take place. This will occur at a voltage on the order of

$$V \approx \frac{L U_i}{e \ell} \quad (32)$$

where V is the voltage across the electrodes separated by length ℓ . L is the mean free path, U_i is the ionization energy, and e is the electric charge.

Generation of electrons (ions) in this manner is called Townsend ionization. This process was discussed earlier. Self-sustained discharge due to the Townsend process is shown as the "normal" region of the I-V characteristic, Figure 2.

At the onset of the Townsend ionization, the discharge current increases as a result of increased electron density.

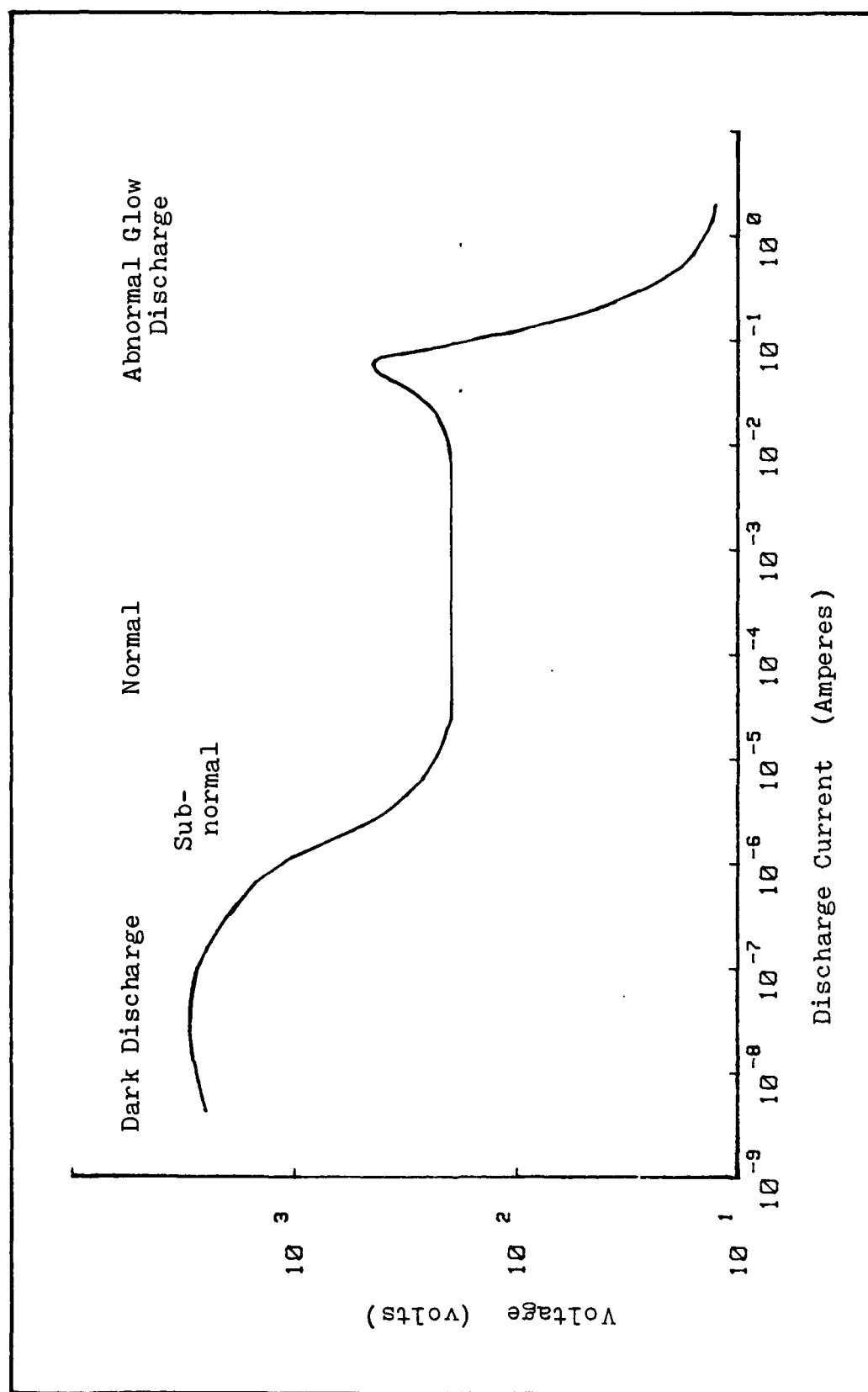


Figure 2. Discharge Current-Voltage Curve

After Townsend ionization begins, the conductivity of the discharge increases resulting in a lower voltage drop across the discharge for the same current.

$$j = \frac{\sigma E}{e} \quad (33)$$

A low resistance non-Townsend discharge can exist if there is an external source of ionization. A glow discharge, similar in appearance to a self-sustained discharge, can exist if the external ionizing source is strong enough. In the externally sustained discharge, when the source is removed, current ceases even though voltage is still applied to the electrodes.

An external source may take the form of ionizing radiation, electron beams, or radio frequency electric fields. Ionizing radiation from radioactive sources is probably the simplest mechanism for externally sustaining a discharge. The problems associated with handling nuclear sources make use in a switch difficult to justify. In addition, these sources cannot be turned off and on easily.

Excitation of a discharge by electron beams and microwaves (RF) can be contrasted not only by the complexity of the sources but by the ionization processes involved. The electron beam uses a high energy stream (flux) of electrons to supply the charge carriers in the discharge through ionization of the neutral gas particles. The high energy primary (beam) electrons impact gas particles at some collision probability P_c (depends on the energy). The secondary electrons at lower energy (higher P_c) impact other particles producing

more secondary electrons. As the collisional process continues, the electron number density increases and the energy distribution moves toward lower energies, a kind of trickle down in energy.

Microwave excitation of a discharge begins by accelerating background electrons in the RF electric field. If the mean free path is long enough (low pressure) that the electron can take on energies that are greater than the ionization energy, the gas ionizes readily. At higher pressures and shorter mean free paths, the microwave fields have to pump up the energy of the electrons through less frequent collisions that result in increased electron energies, or the energy can go into producing metastable excitation. These metastables are more easily excited by the lower energy electrons. The microwave excited discharge was a lower electron energy distribution that is pumped up to ionization energies as opposed to the trickle down for the electron beam discharge. Some of the physical processes which must be optimized in a high repetition rate opening switch depend on such details as the electron energy distribution.

In a microwave excited discharge, the electron production rate must equal the loss rate. The primary loss considerations are (depending somewhat on geometry and plasma density) radial diffusion to the discharge tube walls, recombination, and current in the external circuit. For the geometry of this experiment, diffusion losses are assumed to dominate. The rate of change of electron density is

$$\frac{d n_e}{dt} = \left(\nu_i - \frac{D_a}{\Lambda^2} \right) n_e - R n_e^2 \quad (34)$$

where ν_i is the microwave production rate and D_a/Λ^2 is the electron diffusion rate.

For the steady state and the dimensions of this experiment.

$$\nu_i \approx \frac{D}{\Lambda^2} = \frac{3 \times 10^3}{(.353)^2} = 2.4 \times 10^4 \text{ sec}^{-1} \quad (35)$$

With this method of pumping up the electron's energy, a greater portion of the microwave energy is lost in inelastic collisions and gas heating that does not result in ionization. This reduces the efficiency.

Low Pressure Glow Discharge

The conduction of DC current in a cold cathode discharge requires that there be a production of conduction electrons at the cathode and that they be collected at the anode. The structure of the discharge between the anode and cathode electrodes is divided into regions (Figure 3). These regions are formed as the discharge satisfies the electric field requirement for the current continuity.

The cathode sheath is a region which is formed to generate the electrons to satisfy continuity at the cathode. Electrons are formed at the cathode primarily through positive ion bombardment. A strong electric field is required to give

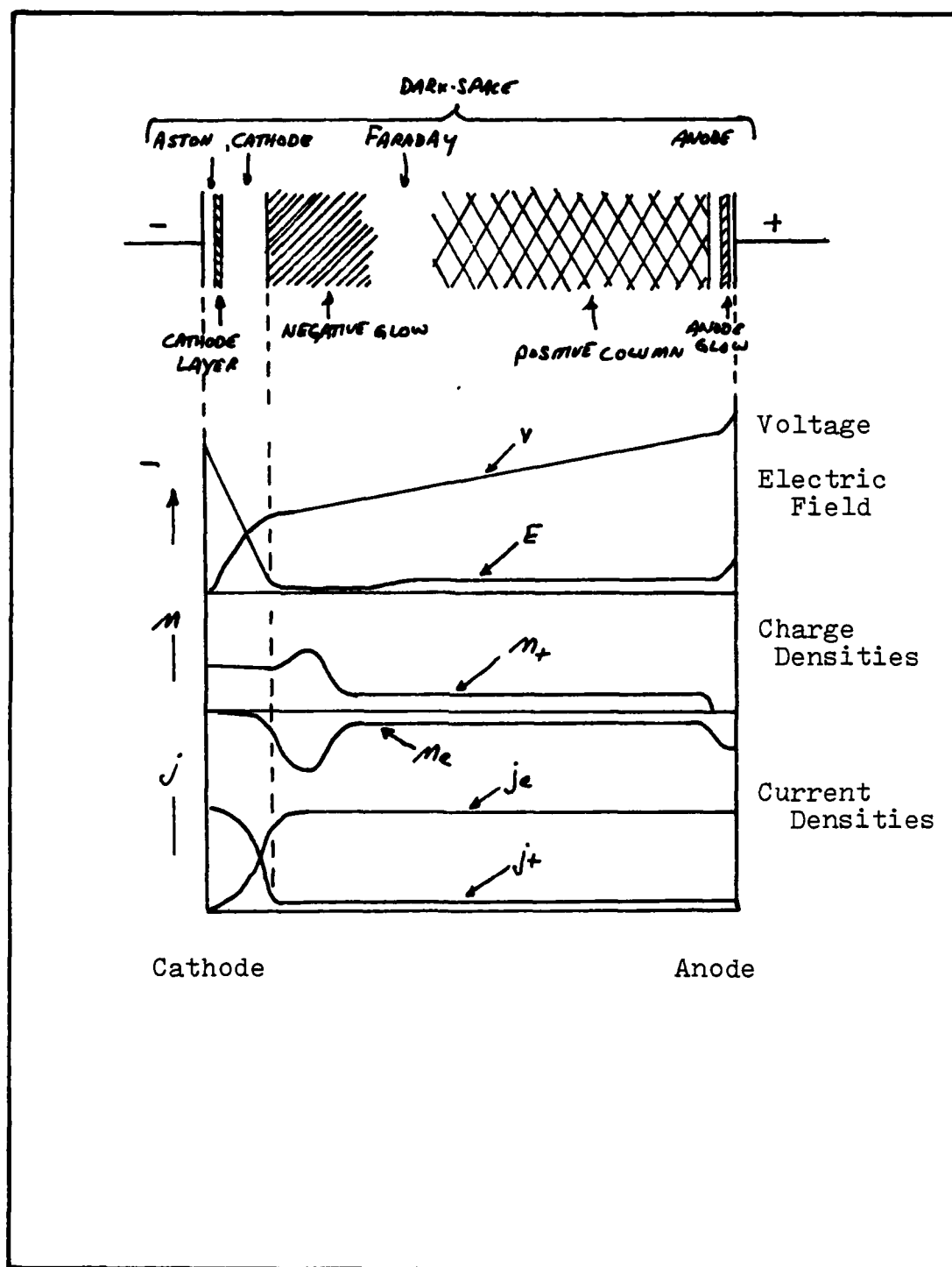


Figure 3. Regions of a Glow Discharge

the ions sufficient energy to generate electrons at the cathode. The electrons produced at the cathode are accelerated through the region known as the Aston dark space by the strong negative field. As the electrons gain energy, some ionize atoms in the cathode region generating electron-ion pairs. The electrons move toward the anode while the ions move toward the cathode to generate more electrons. The electrons are swept out of the high field cathode region. Loss of these electrons from the cathode region leaves a net positive charge in that area. This positive ion concentration acts to decrease the field as the distance from the cathode increases, reducing the electron drift velocity. The thickness of the cathode sheath is determined by the electric field requirements for the production of electrons at the cathode.

There are a large number of electrons produced in the cathode sheath by Townsend ionization which are rapidly accelerated out of this region. Once these electrons are in the reduced field region, they slow down through collisional losses and their number density is reduced through recombination and diffusion. Recombination reduces their number to near that of the background of ions at the beginning of the positive column.

The positive column is a region of little or no net charge. The electric field requirements for this region are only that it be great enough to produce sufficient ionization to replace the electrons lost to diffusion to the walls and, to a smaller degree, losses due to recombination. Due to the

low fields required to maintain the positive column, it can be quite long in extent. In contrast, the sheath regions are determined by the boundary conditions and their dimensions are constrained to the electrode areas.

At the anode, electrons are attracted and the positive ions are repelled. This gives rise to a negative space charge in front of the anode. This produces an increase in the electric field at the anode and a potential drop across this region.

In a cold cathode discharge, the electron production requirements at the cathode demand the highest electric fields. For this reason, the voltage drop across the cathode sheath can be orders of magnitude greater than the remaining portion of the discharge. The luminous and the dark regions of the discharge are clues to the processes that are going on, and are strongly related to the electron energy in that region.

Model I

This model is a simplistic model which should provide a basis for interpreting current-voltage characteristics and showing the relationship between drift velocity and the reduced electric field, E/N . From the voltage across the discharge tube and the gas pressure in the tube, along with the separation of the electrodes, the reduced electric field can be found. This takes the form

$$\frac{E}{N} = \frac{V/L}{2.687 \times 10^{19} \left(\frac{P}{760} \right) \left(\frac{273}{T} \right)} = \frac{V}{L(3.2 \times 10^{16})} \frac{V \text{ cm}^2}{\text{tor}} \quad (36)$$

where V is the voltage across the electrodes, p is the pressure in torr, and T is the temperature (room temperature is assumed).

The current flow in the discharge tube, as measured in the external circuit, is a function of the electron density (n_e), electrode area (A), and drift velocity (W).

$$I = n_e e W A \quad (37)$$

where e is the electronic charge.

If the plasma is uniform, n_e is constant. This means that the current depends only on the drift velocity. If the pressure is constant, the value of E/N will vary directly with the applied voltage. The current flow through the discharge will be a constant times the drift velocity, $I = CW$. The change in current with E/N will be directly proportional to the change in drift velocity with E/N .

This model is based on the following assumptions:

1. Uniform plasma.
2. Negligible sheath effects.
3. Mean free path that is much smaller than the plasma dimensions.
4. Electron production rate provided by the microwaves is much greater than the rate of loss by conduction.

The uniformity of the plasma is necessary to ensure that the relationship between drift velocity and current remain as in equation (37). If the ionization is not uniform in the discharge, the electron number density will also not be

uniform. If n_e becomes a complicated function over the discharge volume, the simple relationship between current and drift velocity is no longer valid.

If a cathode sheath is present, the large voltage drop across this sheath required to maintain current flow makes this model unusable. With a discharge divided into a cathode sheath, positive column, and anode sheath, there is a voltage distribution (large drop across the cathode sheath) which does not permit determination of the electric field within the scope of this experiment. Consequently, if there is a drift velocity dependence on the electric field, it may be impossible to extract. The problem of sheaths will be dealt with in Model II.

For the drift velocity of the electrons in the gas to be a function of both the electric field and collisions, the mean free path must be much smaller than the separation of the electrodes. If an electron could be accelerated from one electrode to the other without undergoing many collisions, the electric current would not be affected by the collisional process.

For argon and helium the elastic collision probability is found from Brown (Ref 18:23) from which the mean free path is found for 0.5, 1.0, and 4.0 torr.

A background of free electrons is necessary to maintain the discharge. This is due to the ionization mechanism of the microwave energy. The ionization rate is dependent on both the strength of the electric field and the electron

Table 1
Collision Probability for Argon and Helium

Argon			
	0.5 torr	1 torr	4 torr
$P_C = 83$ at 12eV	$\ell = .024\text{cm}$.012cm	.003cm
4 at 1eV	0.5	0.25	.063
1.5 at .5eV	1.33	0.67	0.17
3 at .25eV	0.67	0.33	.083
Helium			
$P_C = 20$ 0-10eV	$\ell = 0.1\text{cm}$	0.05cm	.013cm
where $\ell = 1/pP_C$			

density as was pointed out earlier. It is necessary, then, to keep the electron density high enough to maintain the plasma. If the current flow were very high, loss of electrons due to conduction would cause a subsequent reduction in the electron density in the plasma, weakening it. This would result in an increase in the plasma resistance, lowering the current. A balance is then created between the microwave ionization rate and current. In order to have current (drift velocity) depend only on voltage and not the source term S , the ionization rate must be much greater than the electron loss rate due to conduction.

Model II

If the simplistic model just described is not the case and there are different regions in the discharge, it is

expected that the electric field may not be uniform along the axis of the discharge. If this is the case, erroneous conclusions may be drawn as to the magnitude of the drift velocity from the I-VC if this effect were not considered. Lowke and Davies discuss gas discharges in which the space charge effects of the cathode and anode sheath regions in the discharge are significant (Ref 8:4991). Lowke and Davies characterized the three regions in the discharge (cathode sheath, positive column, and anode sheath) in their theoretical analysis. Their analysis was for a discharge that consisted of an externally sustained source of electron-ion pairs between parallel plate electrodes. One case, with conditions as found in a gamma ray ionization chamber, resulted in a sheath thickness that was greater than the electrode spacing and showed only small space charge effects. The electric field was nearly uniform and could be approximated by the applied voltage divided by the electrode spacing. The analytic solution for the current in this case where the sheath thickness (b) is greater than the electrode separation (d), reaches a saturation point that is directly proportional to the source term.

$$I = A e d S \quad (38)$$

where I is the current, e is the electronic charge (1.6×10^{-19}), A is the electrode area, d is the electrode separation and S is the source term ($1/\text{cm}^3/\text{sec}$).

In contrast to this first case, conditions more appropriate for switching were considered by them using higher source functions and discharge currents. The solutions for these conditions were like the characteristic regions of a self-sustained discharge. There was always a plasma region ($n_e \approx n_+$) with a small electric field compared to the high fields present in the sheath regions. Figure 4 is similar to Lowke and Davies' Figure 6 that shows the results of calculations for the charge densities, current densities, and electric field for a current density of 0.254 ma/cm, $S = 3.6 \times 10^{16}$ ion pairs/cm³/sec, and with the electron diffusion coefficient equal to the longitudinal diffusion coefficient (Ref 8:4996). Of particular interest in this figure is the decay to almost zero of the electron density within the sheath due to longitudinal diffusion. The significance of this will be discussed later. An increase in the applied voltage and current density resulted in an increase in the cathode sheath size and significant increases in ionization. The ionization leads to an increase in the positive ion density in the sheath but the electron density still decays as before. Their results show a continued increase in the discharge current with applied voltage.

$$I = A(4\mu e e^3 S^3)^{1/4} V_c^{1/2} \quad (39)$$

(Ref 8:4997, 4999)

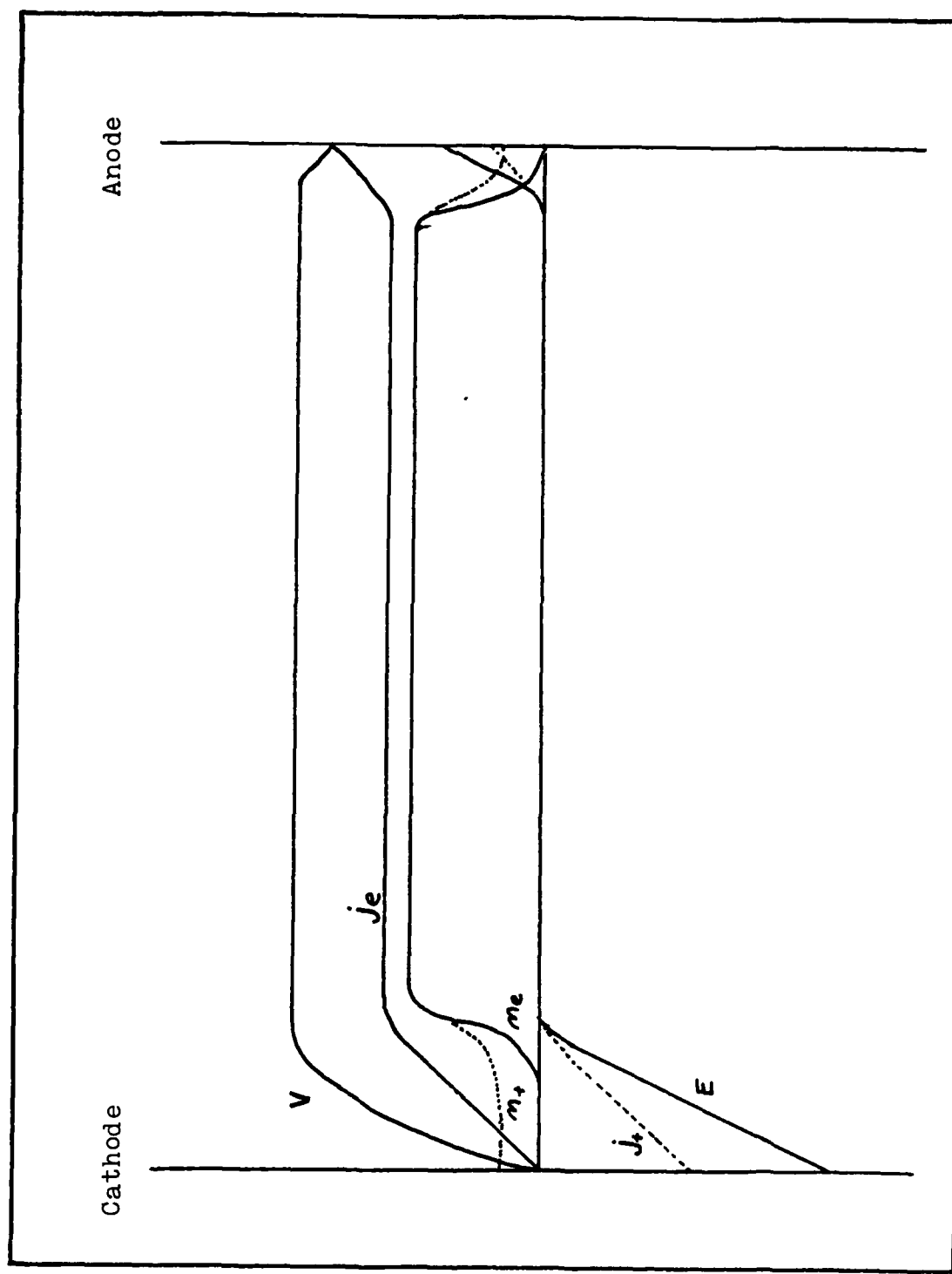


Figure 4. Analytic Model of an Externally Sustained Discharge (Ref 9:48)

The discharge used in this experiment relies on an external source of ionization in a manner similar to that used in Lowke and Davies' calculations (Ref 8:4991). Their electron-ion production sources were gamma rays which produced photo-ionization, nuclear fission fragments, or electron beams which provided impact ionization. The production rates due to these sources depend upon the neutral atom density and the cross-section for ionization.

Ionization using microwaves, on the other hand, comes from electron-neutral (or metastable) impact where the electrons are accelerated by the microwave fields. While the energy source is external, as in the previous cases, the production function will depend on the electron density as well as the neutral density and cross-sections. Referring to Figure 4 from Lowke and Davies (Ref 8:4495), the electron density is not uniform in the cathode sheath and appears to fall off exponentially toward the cathode.

$$n_e = n_{e0} \exp(-x/\Lambda) \quad (40)$$

where $n_{e0} \cong n_{+0}$ and is the electron-ion density of the "positive column" at the cathode sheath boundary, and Λ is a characteristic length shown later to be equal to $D/|W|$.

The source term becomes

$$S = \nu_i n_e \quad (41)$$

where Λ_i is the microwave ionization rate and n_e is the electron density.

$$v_i = \frac{e \bar{E}_{\mu wave}^2}{m U_i v_m} \left(\frac{v_m^2}{\omega^2 + v_m^2} \right) \quad (42)$$

(Ref 21:6)

where e is the electronic charge, $E_{\mu wave}$ is the electric field due to the microwave energy, m is the mass of the electron, U_i is the ionization energy, ω is the angular frequency of the microwaves, and v_m is the collisional frequency. The effectiveness of the electric field in transferring energy to the electrons is embodied in the term

$$E^2 \left(\frac{v_m^2}{v_m^2 + \omega^2} \right) \quad (43)$$

which was introduced earlier.

In order to obtain an analytic solution of the voltage-current relationship, the spatial variation of the discharge parameters are found beginning with continuity equations for electrons and ions and Poisson's equation. The continuity equations are:

$$\frac{dn_e}{dt} = S + n_e \alpha |W| - R n_e n_+ - \frac{dj_e}{dx} \quad (44)$$

$$\frac{dn_+}{dt} = S + n_e \alpha |W| - R n_e n_+ - \frac{dj_+}{dx} \quad (45)$$

where n_e and n_+ are the electron and ion densities respectively, t is time, S is the source function, x is the distance from the cathode sheath-positive column boundary (increasing toward

the cathode), α is Townsend's first ionization coefficient, W is the electron drift velocity, and R is the recombination coefficient. Here, the time rate of change of the electron (ion) density is equal to the production rate by the source term (S) and ionization ($\alpha n_e |W|$) minus the losses due to recombination and electron (ion) flux. The electron and ion flux densities are given by

$$j_e = -n_e |W| - D_L \frac{dn_e}{dx} \quad (46)$$

$$j_+ = \mu E n_+ \quad (47)$$

where D_L is the longitudinal electron diffusion coefficient.

The potential, V , between the electrodes comes from Poisson's equation

$$\frac{d^2 V}{dx^2} = \frac{e}{\epsilon} (n_e - n_+) \quad (48)$$

and the electric field is given by

$$E = -\frac{dV}{dx} \quad (49)$$

The above equations are based on the assumptions that the medium between the electrodes is uniformly ionized by the source function and that the ionization rate by the source is independent of the applied electric field. In addition, processes involving Townsend's second coefficient which allow for production of secondary emission electrons at the electrodes are not considered. Instead, the electrodes are

considered to be perfect absorbers of electrons or ions but not emitters. Figure 5 shows the sign conventions for the following analysis.

If only steady state solutions to the equations above are considered, they become

$$\frac{dj_e}{dx} = S + n_e \alpha |W| - R n_e n_+ \quad (50)$$

$$\frac{dn_e}{dx} = \frac{n_e W}{D} - \frac{j_e}{D} \quad (51)$$

$$\frac{dj_+}{dx} = S + n_e \alpha |W| - R n_e n_+ \quad (52)$$

$$\frac{dE}{dx} = \frac{e}{\epsilon} (n_+ - n_e) \quad (53)$$

$$\frac{dV}{dx} = -E \quad (54)$$

If we consider Equation (52), assuming negligible effects due to ionization (α) and recombination R , use the microwave source term S from Equation (41), and include the positional dependence with the sheath of the electron density Equation (40), this becomes

$$\frac{dj_+}{dx} = \gamma_i n_e = \gamma_i n_{e0} e^{-(b-x)/\lambda} = \gamma_i n_{e0} e^{-b/\lambda} e^{x/\lambda} \quad (55)$$

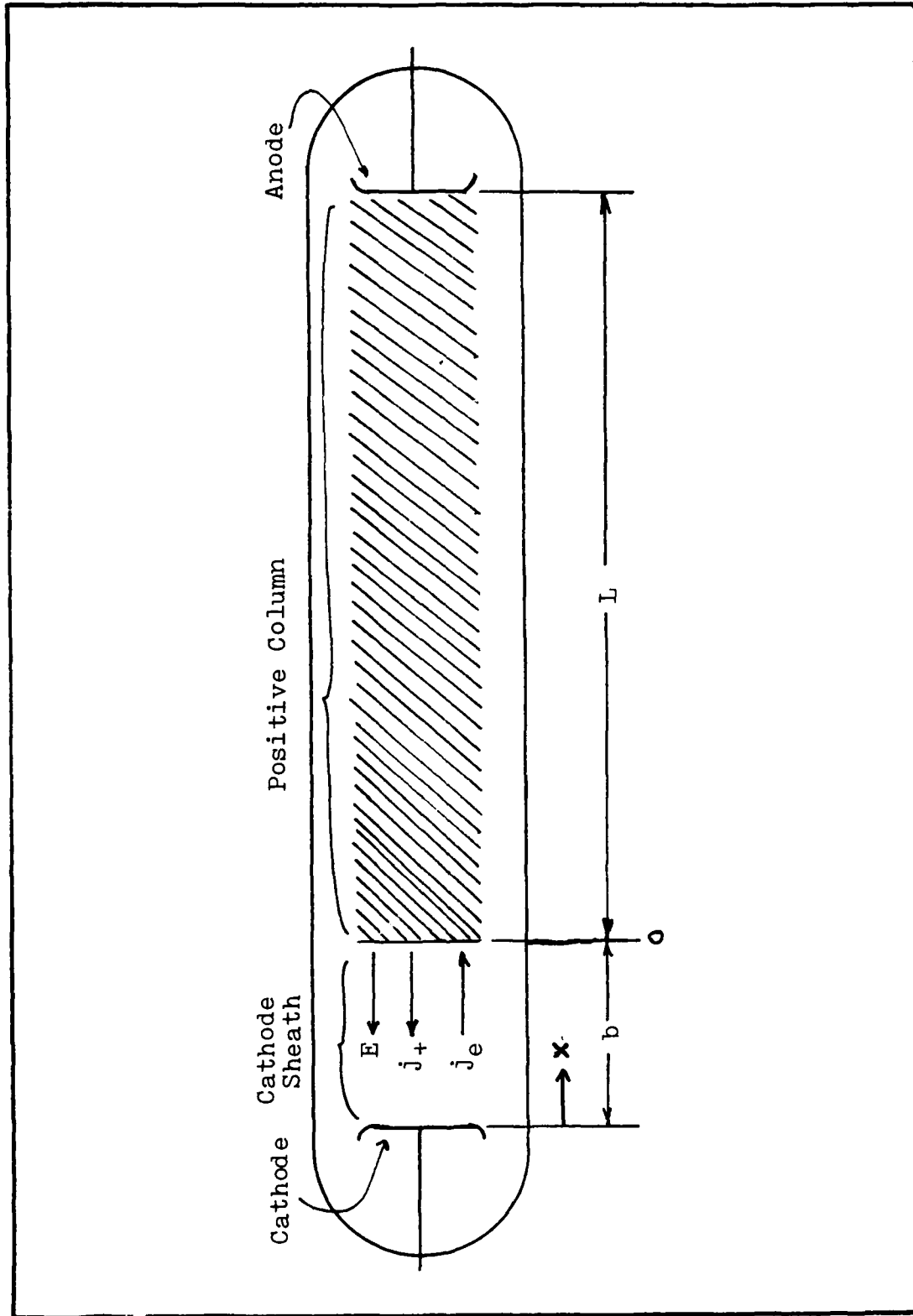


Figure 5. Model II Sign Conventions

Integrating to find $j_+(x)$

$$j_+ = v_i m_e e^{-b/\lambda} \int_0^x e^{x/\lambda} dx = -v_i m_e \lambda [1 - e^{-(b-x)/\lambda}]$$

$$\text{note } j_+(x) = 0 \text{ @ } x=b \quad (56)$$

$$j_+(0) = j_{+0} = -v_i \lambda m_e \text{ @ } x=0$$

substituting this expression for j_+ in Equation (47) and substituting this and Equation (40) into Equation (53) and considering only longitudinal variations in electric field it becomes

$$\frac{dE}{dx} = \frac{e}{\epsilon} \left[\frac{|j_+|}{\mu E} - m_e e^{-b/\lambda} e^{x/\lambda} \right] \quad (57)$$

$$\frac{dE}{dx} = \frac{e m_e}{\epsilon} \left[\frac{v_i \lambda}{\mu E} (1 - e^{-(b-x)/\lambda}) - e^{-(b-x)/\lambda} \right] \quad (58)$$

This differential equation can be analyzed a little easier by making the assumption that the cathode sheath thickness b is much greater than the characteristic length λ . For a thick sheath and short diffusion length, $x \gg \lambda$, then it follows from Figure 4 that $n_+ \gg n_e$ and we can neglect the contribution of n_e to the electric field. Equation (57) becomes

$$\frac{dE}{dx} = \frac{e}{\epsilon} \frac{j_+}{\mu E} = \frac{e m_e}{\epsilon} \frac{v_i \lambda}{\mu E} (1 - e^{-(b-x)/\lambda}) \quad (59)$$

$$E dE = \frac{e m_e v_i \lambda}{\epsilon \mu} (1 - e^{-(b-x)/\lambda}) dx \quad (60)$$

and integrating to find E

$$\int E dE = \frac{e m_e v_i \lambda}{\epsilon \mu} \int_0^x (1 - e^{-(b-x)/\lambda}) dx \quad (61)$$

$$E^2 = \frac{ze M_{e0} V_i \Lambda}{\epsilon \mu} \int (1 - e^{-(b-x)/\Lambda}) dx \quad (62)$$

Again for $x \gg \Lambda$, $e^{-(b-x)/\Lambda} \ll 1$

$$E^2 = \frac{ze M_{e0} V_i \Lambda}{\epsilon \mu} x \quad (63)$$

$$E = \left(\frac{ze M_{e0} V_i \Lambda}{\epsilon \mu} \right)^{1/2} x^{1/2} \quad (64)$$

Since the voltage across the cathode sheath is the integral of E over the length of the cathode sheath

$$V_c = \int_0^b E dx \approx \int_0^b \left(\frac{ze M_{e0} V_i \Lambda}{\epsilon \mu} \right)^{1/2} x^{1/2} dx \quad (65)$$

$$V_c \approx \left(\frac{ze V_i M_{e0} \Lambda}{9 \epsilon \mu} \right)^{1/2} b^{3/2} \quad (66)$$

Since the cathode is not considered to be an electron emitter and the electron density approaches zero near the cathode, current at the cathode is assumed to be only due to the positive ions j_+ . Substituting in the current equation, $I = ej_+ A$, Equation (56) for j_+ and evaluating at $x = B \gg \Lambda$, $x = b \gg \Lambda$, the result is

$$I_{SAT} = e A j_+ \Big|_{x=b} = e A V_i M_{e0} \Lambda \quad (67)$$

For a cathode sheath where $b=x \gg \lambda$, the current reaches a saturation value. This saturation is proportional to the strength of the source term. Saturation current only occurred for Lowke and Davies for the case of very weak sources, where the cathode sheath b was greater than the electrode separation (Ref 8:4995).

Analyzed at the other limit where $b < \lambda$ implies that x is also less than λ . From Equation (40), this means that free (conduction) electrons exist all the way to the cathode. Under these conditions the cathode sheath lacks the definition it has when $b \gg \lambda$. When $b < \lambda$, the voltage drop across the sheath is much less than the drop across the positive column, and Model I applies.

The depletion of electrons in the cathode sheath region due to the electric field is in competition with diffusion, which tends to keep the electron density uniform. The value of the characteristic length λ , then, should be proportional to the electron diffusion coefficient and inversely proportional to the electron drift velocity.

$$\lambda \propto \frac{D}{W} \quad (68)$$

This result is found analytically by rearranging Equation (51) and substituting $-\frac{1}{\lambda} n_e$ for dn_e/dx and using the absolute value of W with a negative sign for the term $n_e W$

$$j_e = -n_e |W| + \frac{D}{\lambda} n_e \quad (69)$$

and with

$$j_{\text{TOTAL}} = j_+ - j_- \quad (70)$$

where j_+ is found in Equation (56) and j_{total} is evaluated at $x = 0$ (the electrode). Substituting these into Equation (70)

$$(|w| - D/\Lambda) n_{e0} e^{-(b-x)/\Lambda} = v_i n_{e0} \Lambda e^{-(b-x)/\Lambda} \quad (71)$$

canceling terms

$$|w| - D/\Lambda = v_i \Lambda \quad (72)$$

which becomes

$$\Lambda^2 - \frac{|w|}{v_i} \Lambda + \frac{D}{v_i} = 0 \quad (73)$$

Solving for Λ

$$\Lambda = \frac{1}{2} \frac{|w|}{v_i} \left[1 \pm \sqrt{1 - \frac{4Dv_i}{w^2}} \right] \quad (74)$$

For a real solution, it is necessary to assume the negative root, and recognizing that $4Dv_i/w^2 \ll 1$, this reduces to

$$\Lambda = \frac{D}{|w|} \quad (75)$$

The fact that Λ does not depend on the microwave ionization rate is reassuring. This characteristic length represents a ratio between diffusion due to the concentration gradient and the force pulling the electrons to the anode by the electric field which is embodied in the drift velocity, Equation (68).

III. Equipment

The equipment used in this experiment was configured to provide a near uniform microwave excited discharge in a high purity flowing gas in which the current-voltage characteristics (I-VC) could be determined. For purposes of explanation the equipment will be described in subsections. Microwave sources supplied the ionizing energy to maintain the discharge in excited state. Various waveguide components were used to couple the microwave energy to the applicator while protecting the sources. The applicator is the device which actually couples the microwave energy to the discharge plasma. The discharge tubes contain the electrodes which provide the DC field used to measure the I-VC. Direct current (DC) sources and diagnostic equipment were used to obtain the plasma characteristics. Discharge tube gas pressure and flow rates (and thereby the purity) were determined for the gas supply and vacuum system. In addition to these, personnel safety was ensured by an interlock system that monitors radiation levels and provides automatic or manual emergency shutdown in case of hazardous microwave leakage or other operator detected emergency.

Microwave Sources

The experiment used two continuous microwave sources and has provisions for the application of pulsed microwave energy from two separate generators. The continuous (CW) microwave sources used were Gerling Moore, Inc. Model 4006

low ripple power sources. The CW generators operate at 2.45 GHz in the industrial microwave band, are capable of 2.5 kilowatts, and have front panel waveguide output. Both CW sources were operated at about 80% of full power to minimize ripple in the output. The power levels actually coupled to the applicators were adjusted by detuning a circulator-dummy load (this will be described in more detail later).

For pulsed operation two Epsco Model PG5KB generators are available which give a peak output of about 4.5 kilowatts. While the CW sources are fixed frequency, the PG5KB can operate over a frequency range of 2.35 to 2.7 GHz with the Model 5238HB8 plugin. The pulse repetition rate can be varied with internal or external control over a range of 20 to 25,000 pulses per second. The pulse width is 0.3 to 50 microseconds with a maximum duty cycle of 0.005 for rated power. The Epsco has a coaxial output.

Any combination of the microwave sources can be used at once. The most uniform discharges, however, seem to come from approximately balanced power from both CW sources.

Microwave Components (Loads, Circulators, and Detectors)

The microwave applicators are connected to the generators by flexible rectangular waveguide (Figure 6). The flexible waveguide and quick connect ring clamps make reconfiguring easier and allow for changes in the relative positions of the applicators.

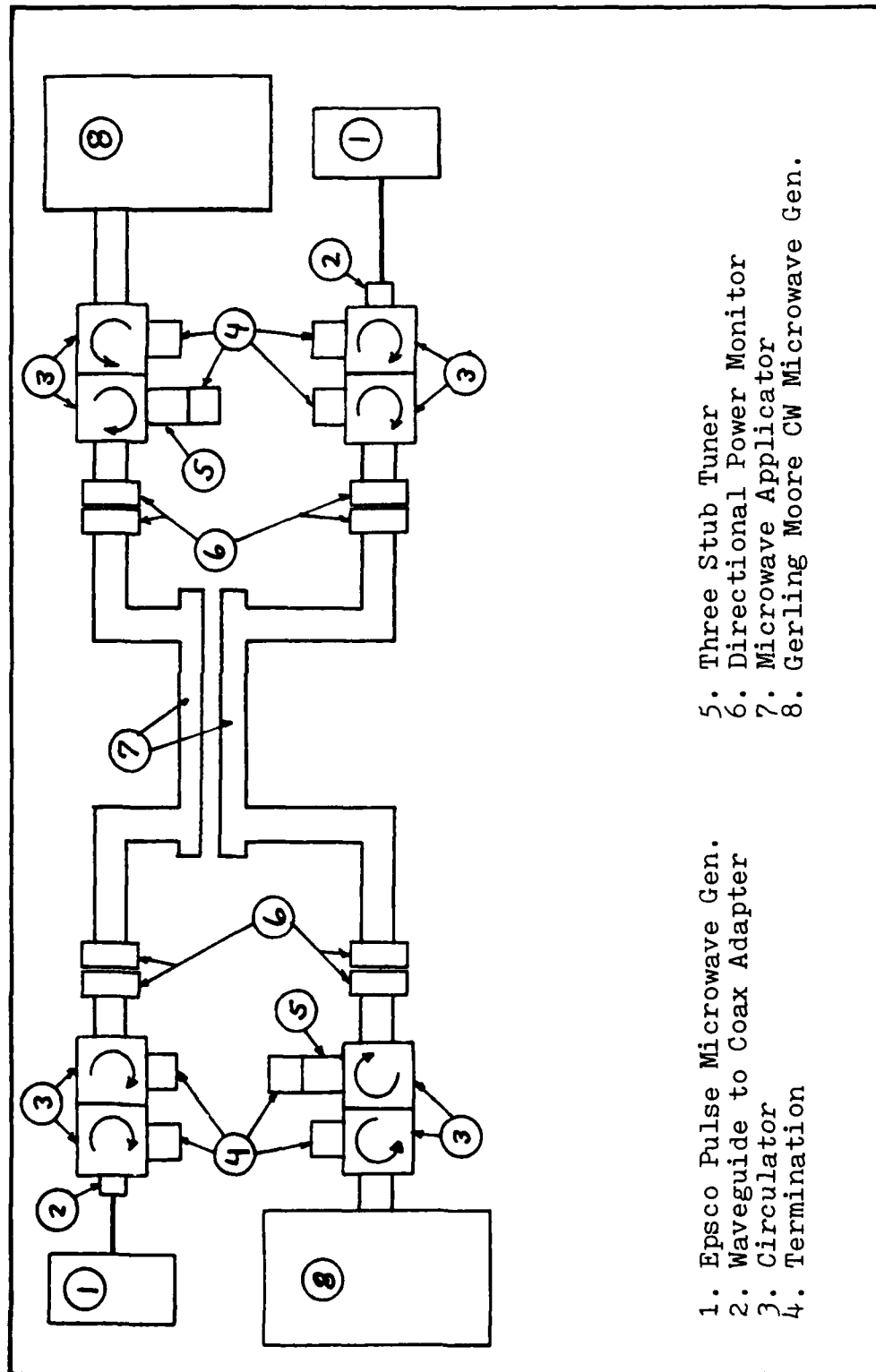


Figure 6. Experimental Arrangement

With the CW generators operating at about 80 percent of peak power and the discharge requiring a relatively small amount of the power, the remaining microwave power must be channeled into dummy loads. On the output of the CW generators are circulators which direct the microwave power into dummy loads via impedance matching sections with three stub tuners. By introducing a mismatch at the dummy load, part of the power is reflected back into the circulator and out to the applicator. With this arrangement, relatively small amounts of power can be directed to the applicator while driving the magnetrons at a higher power level where there is less ripple.

Protecting the CW generators from reflected power are another set of circulators and associated dummy loads. These circulators are placed immediately following those used for power adjustment. The microwave power from the generator is allowed to pass on to the applicator but power reflected (toward the generator) is directed into a dummy load. Microwave power that is not absorbed in the plasma or reflected is transmitted out the other end of the applicator. On the output end of the applicator another circulator-dummy load arrangement is used. Here the unused power from the applicator is dissipated in a dummy load. The third port of this circulator-dummy load has a waveguide to coax adapter that is connected to the Epsco generator for pulsed microwave insertion. Therefore, the

pulsed microwave power is coupled to the applicator while the unused CW power and reflected pulsed power is dissipated in the dummy load.

In order to determine the amount of power that is actually dissipated in the plasma, power incident on each applicator, power through each applicator, and power reflected must be accounted for. These measurements were made using Gerling-Moore detector mounts, Models 4009 and 4010. These are small in line waveguide directional couplers which have about 45 dB of attenuation and 30 dB directivity. The detectors used were Hewlett Packard 420A with point contact diodes. Analog meters, calibrated in scales of 0-1000 and 0-3000 watts, were connected to the H/P 420A detectors. Accuracy claimed by the manufacturer is about 5 percent of full scale for these power monitors. Previous experimenters using this same equipment suggest an accuracy of more like 15 percent of full scale but having a repeatability in settings of 5 percent. The detector mounts are sensitive to mechanical shock which can change the position of the detector probe and thus, its coupling factor. Also, the detector crystals are sensitive to high voltage transients from other equipment such as the tesla coil used to initiate the plasma discharge. Therefore, the accuracy of the meters was checked against local standards (described in the next chapter).

With the magnetrons operating at near maximum power and a relatively small amount of this power deposited in

the plasma, the dummy loads must be cooled to dissipate the unused power. In addition, the CW microwave generators require cooling for the magnetron oscillator tubes. Two single pass, flowing (tap) water circuits are used to cool the magnetrons and dummy loads. The generators are interlocked with coolant flow switches to prevent damage to the magnetrons. A closed cycle cooling circuit is used to protect the three port circulators from overheating. A Neslab Model HX-200 closed cycle heat exchanger pumps and cools the water-Clorox cooling mix. The Clorox is used to prevent algae growth. An additional house water circuit cools the heat exchanger.

Applicator

To couple the microwave energy into the plasma, two identical applicators were used to form a sandwich with the discharge tube in between (Figure 7). The applicators were Gerling-Moore, Inc. Model 4055 interdigital slow wave transmission lines. As the microwave energy travels down the interdigital line, an evanescent field extends away from the surface. It is the evanescent field which interacts with the fill gas in the discharge tube. Since this applicator behaves more like a transmission line than a resonant cavity, which is frequently used to generate intense microwave fields for similar applications, its properties are more broad band (than the high Q resonator) and power which is not absorbed in the load travels to the exit end of the line and is not reflected.

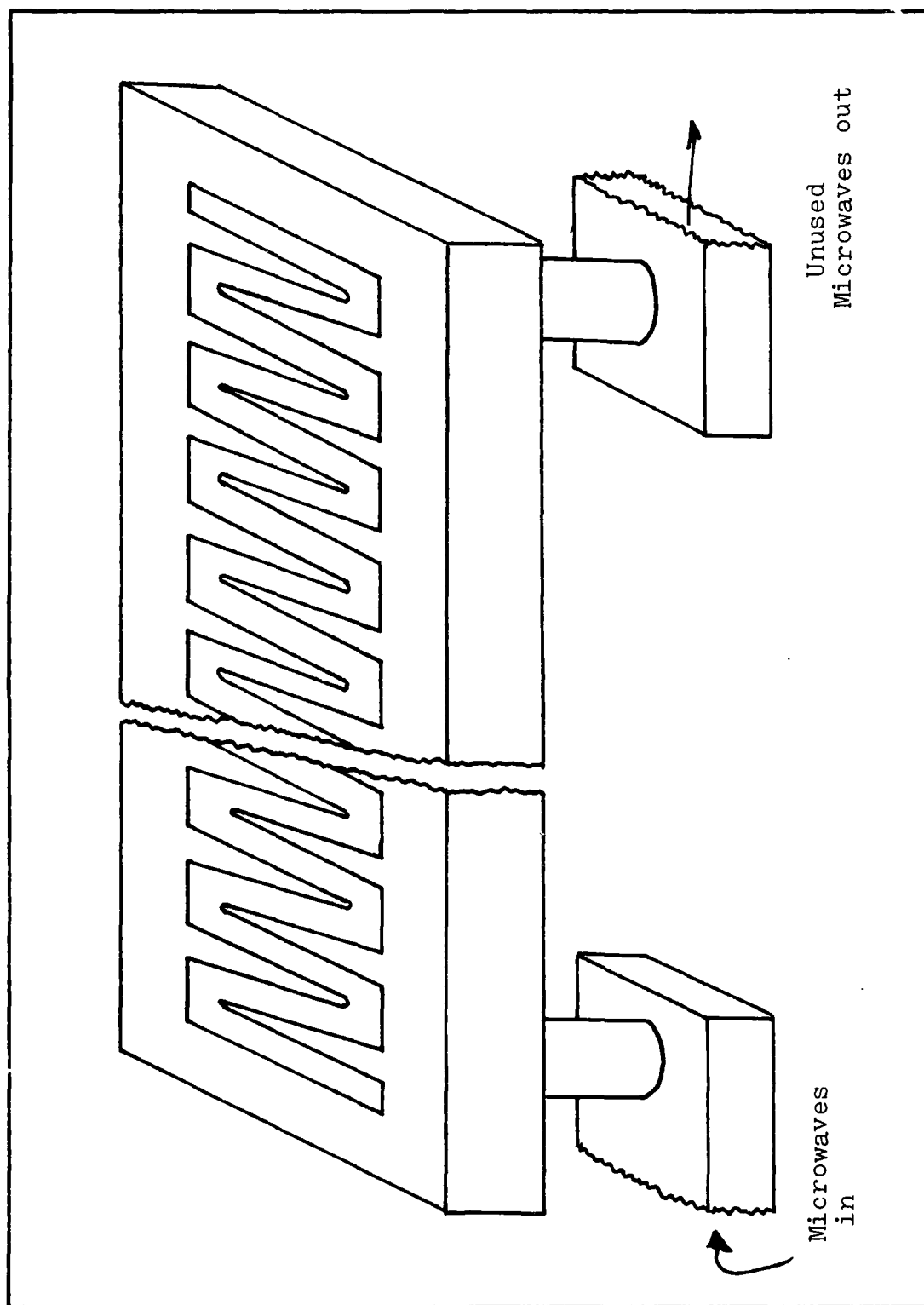


Figure 7. Microwave Applicator

The applicator is constructed of dip brazed aluminum with an active microwave area 1 by 18 inches and has WR 284 waveguide flanges. Operating in the frequency range of 2.4 to 2.5 GHz, it has a maximum power rating of three kilowatts. The manufacturer specifies the field strength to be 5000 volts per centimeter at an input power of 2.5 kilowatts. The fields fall off exponentially to nearly zero at a half wavelength, approximately 10 cm, above the applicator in the free-field condition. At this distance the leakage fields should be less than ten milliwatts per square centimeter (Ref: 23). With the plasma tube sandwiched between the two applicators the free-field conditions are not expected to be valid as the boundary conditions are changed.

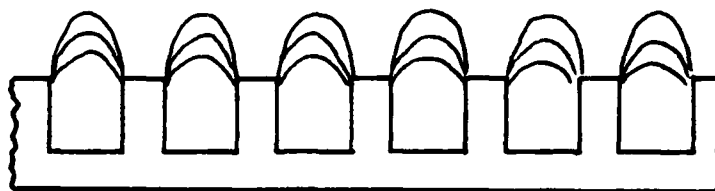
Previous experiments were done by Universal Energy Systems, Inc. and Technology, Inc. using the same applicators. As part of their experiments, the electric fields above the applicators were determined. The fields were measured with a dipole antenna probe. Electric field versus height measurements were taken at many locations along the longitudinal axis of the applicator and the results averaged. Using the breakdown characteristics of helium at various pressures and the field decrease with height from the dipole measurements, the electric field was determined to be 3600 volts/cm at about one millimeter above the applicator with 2.5 kilowatts input.

In the free-field condition, the field distribution would appear as in the cut-away of Figure 8A. If a

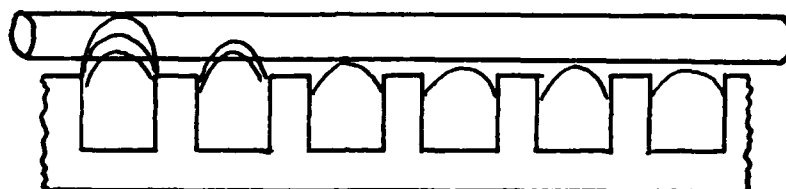
discharge tube is placed in the field, power is absorbed from the first section with a subsequent decrease in power level farther down the applicator, Figure 8B. The fields can quickly fall below the ionization threshold of the gas resulting in a discharge at only one end. To obtain a uniform discharge, the tube must be placed at an angle with respect to the applicator surface. The inclination of the tube should match the reduction in power due to the plasma excitation, Figure 8C. The most uniform discharge was obtained when the two applicators are separated so the discharge tube can be placed at an angle with respect to both of them. In addition, the microwave power from the two separate sources was fed from opposing ends (upper and lower).

Interlock System

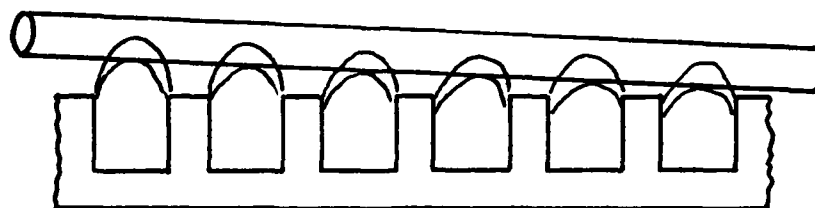
For safety of both equipment and operating personnel, an interlock system was used. If the ambient microwave power in the test area becomes excessive, the interlock system will turn off all of the microwave generators. The master control unit is a Holiday Industries, Inc. Model HI-1500-3 microwave interlock system. The master unit controls a slave unit that contains interrupting relays for the generators. A radiation sensor on the master control unit can open the interlock loop. Also, if the operator should detect a situation requiring immediate microwave shutdown, there is a panic button which will also open the interlock loop.



A. Applicator Free Field



B. Applicator Field With Discharge Tube



C. Field With Inclined Discharge Tube

Figure 8. Applicator Fields With a Discharge Tube

For the protection of the 2.5 kilowatt CW generators, both of their cooling circuits are equipped with flow switches. These switches are in series with the control circuitry and prevent magnetron operation without coolant flow.

As an added precaution against dangerous microwave radiation levels, a portable field intensity measuring test set is available. A Narda Microline Model 8110 electromagnetic radiation monitor, capable of measuring radiation levels down to 2 mW/cm² full scale, is used to sniff out hazardous radiation under operating conditions after a change in configuration is made.

Discharge Tubes

Two styles of discharge tubes were used in the experiments. In both cases the discharge tubes were constructed of quartz with optically clear quartz windows on the ends. The electrodes were between the gas inlet and exit ports with the discharge tube and, therefore, the gas flow, longitudinal or along the axis of the applicators.

The first discharge tube used 14 centimeter electrodes which applied an electric field transverse to the flow of the gas (and applicator). A drawing of this discharge tube with dimensions is in Figure 9A. With the electrode spacing only 0.8 cm, care was taken to reduce field enhancement at the electrode surfaces. The electrodes (aluminum) were cut to approximate a Chang profile (Ref: 23) by machining the central opposing surfaces with two different radii and

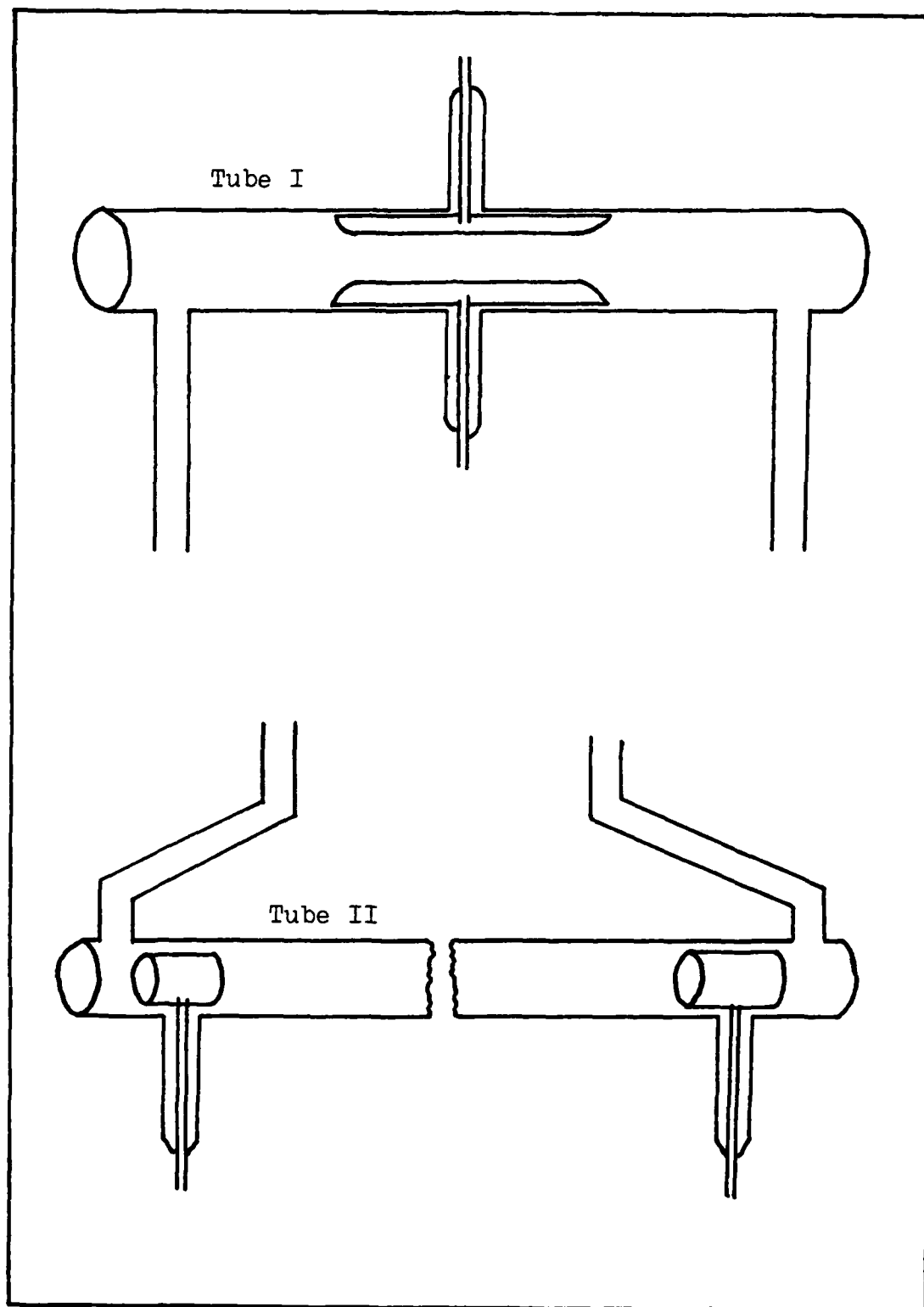


Figure 9. Discharge Tubes

rounding the edges. The ends were hand ground to match a Chang profile template. A back radius to match the discharge tube inner wall located the electrodes and they were held in place by single kovar rods threaded into the electrodes and exiting through graded glass seals.

Early tests showed that aluminum electrodes placed in the applicator fields did not show signs of ohmic heating. During the first series of I-VC runs using pure (tank) helium at 0.5 torr, with 300 watts applied to the applicators, the electrodes began to melt. This initiated the design of the second tube.

The second discharge tube, similar in construction to the first tube (Figure 9B), used 1/2 inch diameter by 2 inch long kovar cylinder electrodes at the ends of the discharge tube. A new quartz tube and windows were required but the graded seals were reused. The electrode separation for this tube is 40.6 cm and special profiles were not used.

Gas and Vacuum System

In order to keep the purity of the fill gas in the discharge tube as high as possible, a flowing gas system was used. Shown in Figure 10, the gas-vacuum system used a metering valve to control the flow and pressure in the discharge tube. Due to the relatively low conductance of the plumbing, flow rate and discharge tube pressure were not independent. For higher pressures (~ 10 torr), it was necessary to throttle the intake line to the mechanical pump to avoid unnecessarily high flow rates. Flow rates were measured with a Hastings Model ALL-500 mass flow

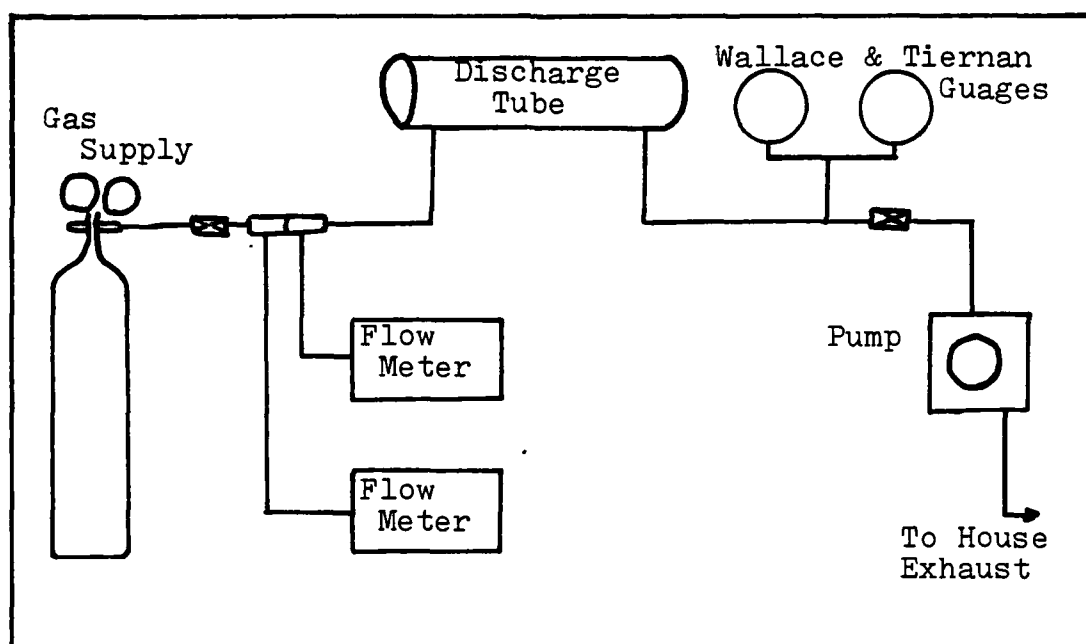


Figure 10. Gas and Vacuum System

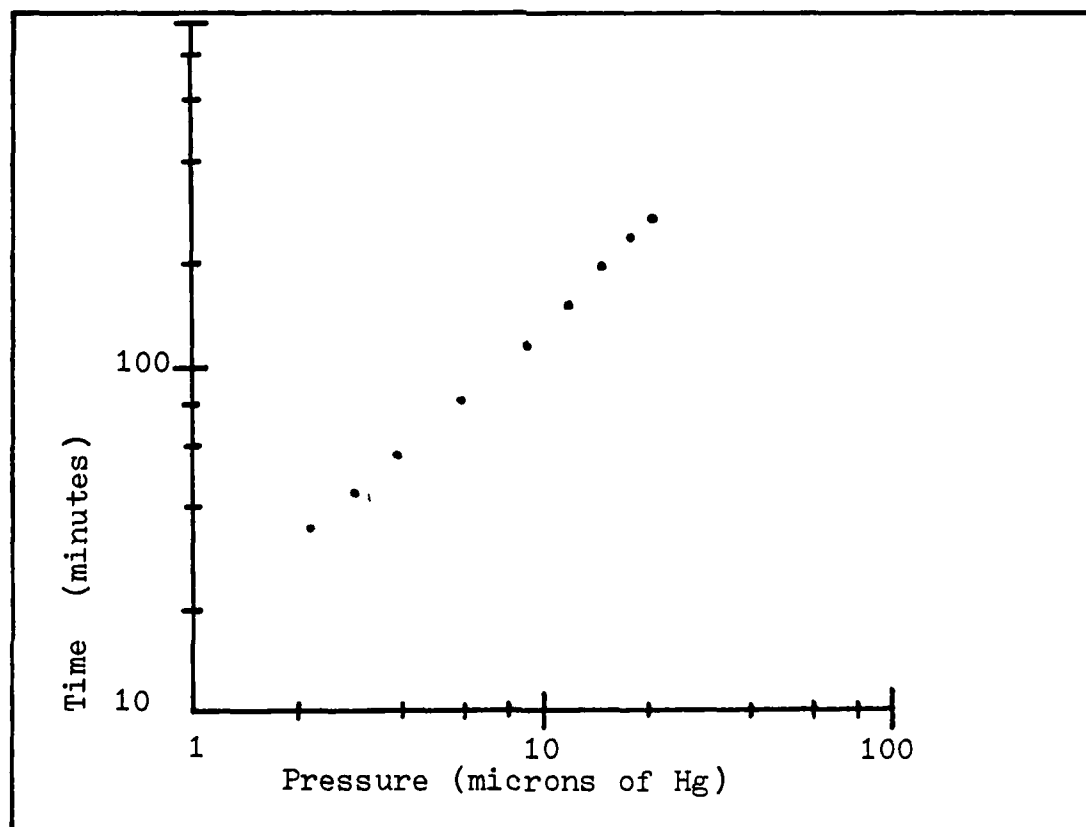


Figure 11. System Leak-up

meter and the pressure was monitored by a Wallace and Tiernan pressure gauge (0.1-20 torr). The Wallace and Tiernan pressure gauge was calibrated against a Baratron gauge and it was found that a +0.25 torr adjustment to the gauge reading was required.

System leakup measurements were made (Figure 11) and the leakup rate was determined to be 1.16 millitorr per min. With this rate, a purity of one part in 10,000 would be maintained at about 3 SCCM and one part in 1000 at 0.3 SCCM. With the discharge tube pressure set for one torr, there was a flow rate of about 5 SCCM.

The gases used for the experiment were all high purity, analyzed gases. The argon-nitrogen mixes were 0.1, 1.0, 9.98 percent nitrogen in argon. Used for comparison and as controls were 1.0 and 10 percent nitrogen in helium, tank helium and pure argon.

DC Source and Diagnostics

For the first discharge tube, DC voltage-current characterization used a slowly varying voltage source and recorded the discharge current as a function of the applied voltage, see Figure 12. The voltage source used was a Wavetek Model 144 HF sweep generator that provided a triangular wave and a Hewlett Packard Harrison 6824A power supply-amplifier. This voltage signal was applied to the discharge tube through a Fluke A90 current shunt that was used to develop a voltage proportional to the plasma

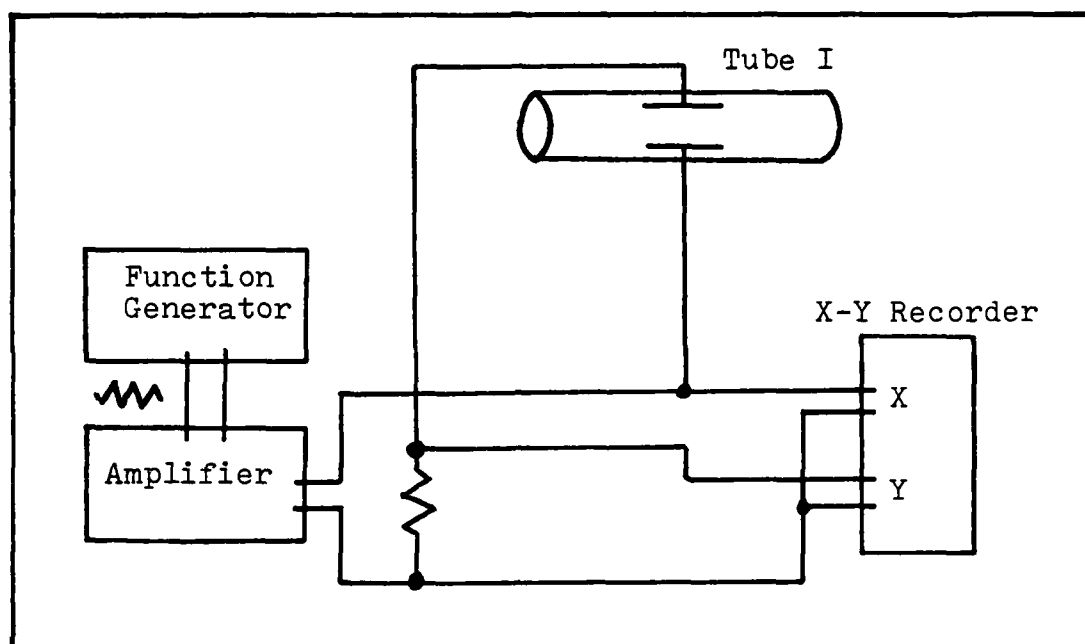


Figure 12. Diagnostics for Discharge Tube I

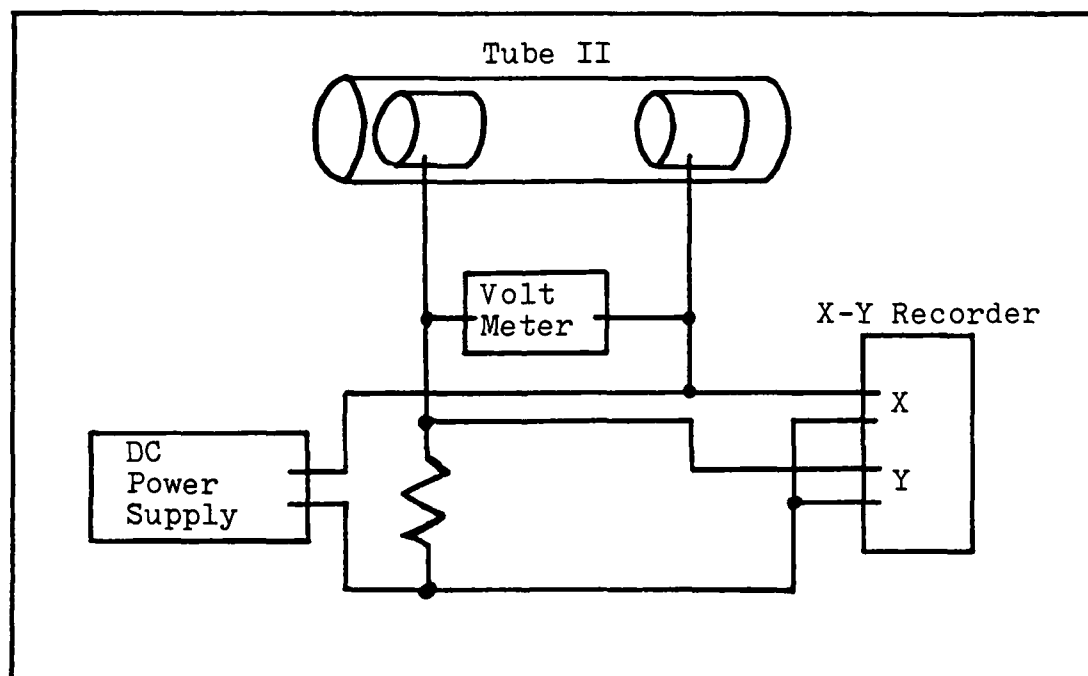


Figure 13. DC Diagnostics for Discharge Tube II

current. A Hewlett Packard 7000 series X-Y recorder plotted the voltage across versus the current through the discharge tube on the X and Y axis, respectively.

The power levels were visually monitored on analog meters, described earlier, but the actual power levels were recorded as diode voltages, read in parallel with the meters. A rotary switch permitted a Fluke Model 2401C integrating voltmeter to access each of the important power monitoring diode detectors. Conversion from the diode voltage readings to power in watts is taken from individual calibration curves for the meters.

With the second discharge tube in place, it was necessary to go to a higher voltage supply as the HP 6824 was limited to plus and minus 50 volts, see Figure 13. An HP 212A replaced the triangular wave generator and amplifier and it was necessary to 'sweep' the applied voltage by hand, slowly rotating the high voltage adjustment. The applied voltage was monitored by a Fluke Model 8000A digital multimeter. The rest of the diagnostics remained the same but at voltages higher than 180 volts, the X-axis sensitivity on the X-Y recorder had to be reduced. A voltage scale was placed on the X-axis for calibration.

Pulsed I-VC measurements were made by using a General Radio Model 1217B pulse generator as a voltage source. Simultaneous voltage and current waveform displays were presented on a Tektronix 556 oscilloscope. While the applied voltage came in through a 1A4 plugin, the plasma

current monitor waveform passed through a 1A7A high gain differential amplifier that was band limited. This provided some reduction of high frequency noise on the current monitor signal. Line synchronization for the pulsed measurements came from another Tektronix 545A oscilloscope. This reduced a considerable amount of current signal amplitude variation due to power fluctuations that resulted from line frequency ripple in the high voltage DC supplies for the magnetrons, see Figure 14.

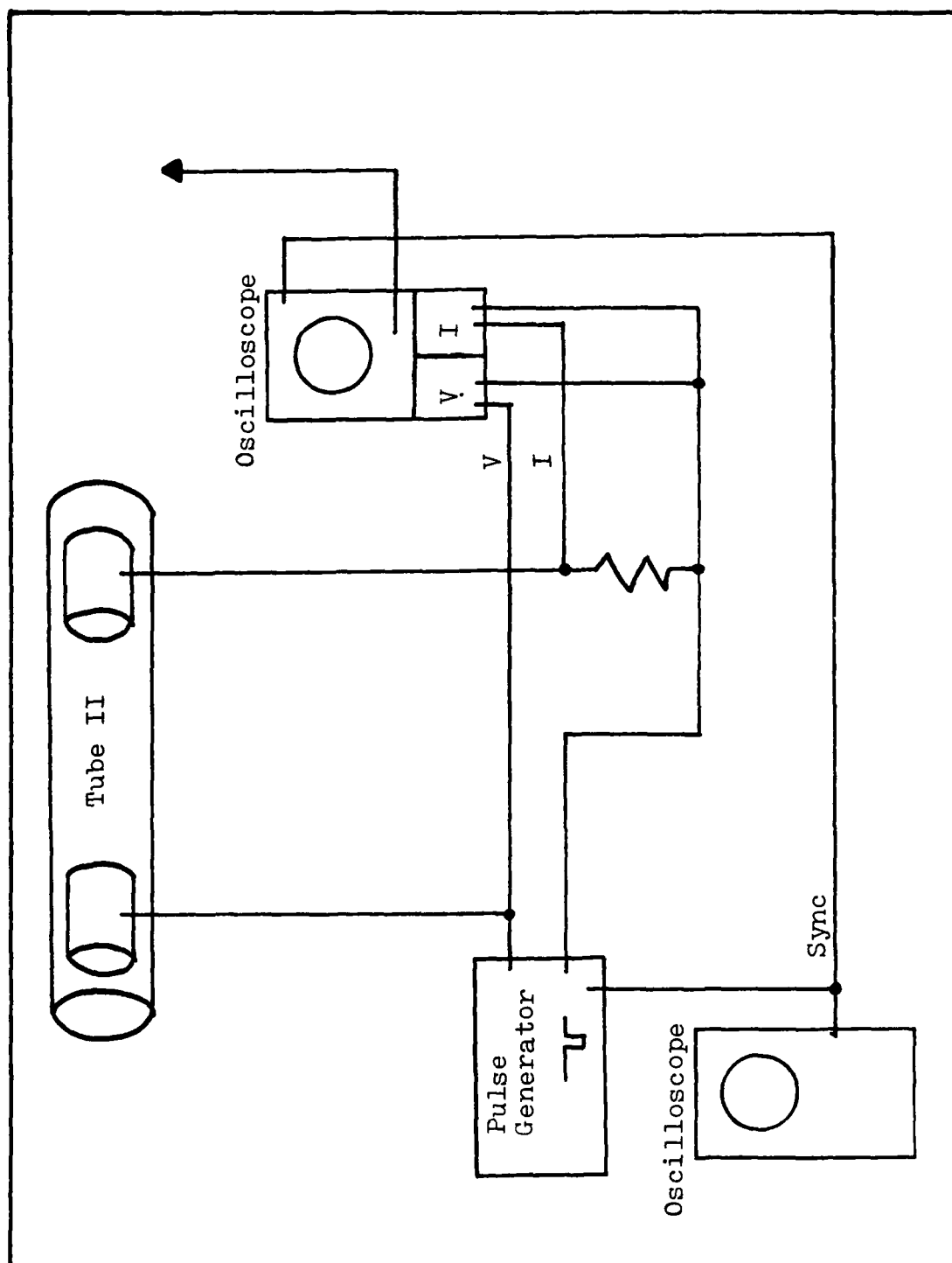


Figure 14. Diagnostics for Pulsed Measurements

IV. Procedure and Results

This section describes the procedures used in this investigation. First, the experimental preliminaries of checking the gas and vacuum system will be described along with the calibration checks for the power meters used in data taking. Following this will be a description of the normal operating procedure. Finally, the methods used to measure the current-voltage characteristics will be presented along with initial and observations that were driving forces in the direction the experiment was to take and the data.

Gas/Vacuum System

The gases used in this experiment were all 'high purity' pure or specified percentage mixtures. This was to reduce the effects of contaminants that may disguise the results that were sought. In order to reduce the amount of contaminants that may be introduced into the discharge tube during a measurement, the system was first made vacuum tight to achieve the best mechanical seals possible with the vacuum components used. Leak up rates were then taken and adjustments were made, as required, to obtain the lowest possible leak up rate. All of the components had not been used for some time so the entire system was pumped on for 72 hours to reduce outgasing. In addition to the components listed in the equipment chapter, it was necessary to add a Hastings Model VT-6 vacuum gauge to the system. It was

possible to achieve a vacuum of 5.5 microns. With the pump sealed off, the pressure was allowed to rise in the system and the increase of pressure versus time is plotted in Figure 11. Calculations were then made to find the minimum flow rate that would be necessary to maintain a purity of one part in 10,000. This flow rate was maintained during the measurements.

Other steps were taken to insure high purity. When a gas cylinder was changed, the fittings were flushed with the new gas prior to sealing the connection between the regulator and the cylinder. After the connection was made, the new gas was allowed to flow through the discharge tube at rates greater than 500 SCCM for two to five minutes before reducing the pressure for measurement. When the system was not in use and the gas was turned off, the vacuum pump was left on to keep leak contaminants down to a minimum.

Microwave Power Meter Calibration

The microwave power meters used in this experiment consisted of Gerling Moore Model 4009 and 4010 detector mounts and meters used with Hewlett Packard 420A detectors. The calibration of the detector mounts can be easily altered by handling and the diodes are subject to degradation by high voltage transients and ground return currents. Also, since the power meters had not been calibrated recently, this calibration check was made.

There were no local standards available that could measure the average power required at the frequency at

which the detectors operate. It was necessary to check the calibration of the meters against one another and use a series of couplers and an attenuator that would be able to reduce the power to a level that could be measured on an HP 431C power meter. The microwave generator used was one of the 2.5kw CW discharge exciters. Figure 15 shows the equipment set up for calibration.

The generator output was coupled to the chain of detectors by two circulators with dummy loads, one tunable. Reflected power from the tunable load was the microwave power used for calibration. At the output of the detector string was a 10 dB HP directional coupler followed by a water load. The 10 dB output from the directional coupler was reduced further by a 20 dB cross guide coupler. The output, now 30 dB below the input level, was attenuated still more by an HP variable attenuator before measurement by the 431C power meter. Unused ports on the couplers were terminated in dummy loads.

The value of power indicated by the detector's meters was monitored by a digital voltmeter and readings were taken at several power levels up to 500 watts. After calibration values had been taken in the forward direction, the detectors were reversed and readings were taken again. This reversal of the detectors provided calibration for the detector mounts that measured both forward and reverse power. Reversing the detectors also gave an indication of

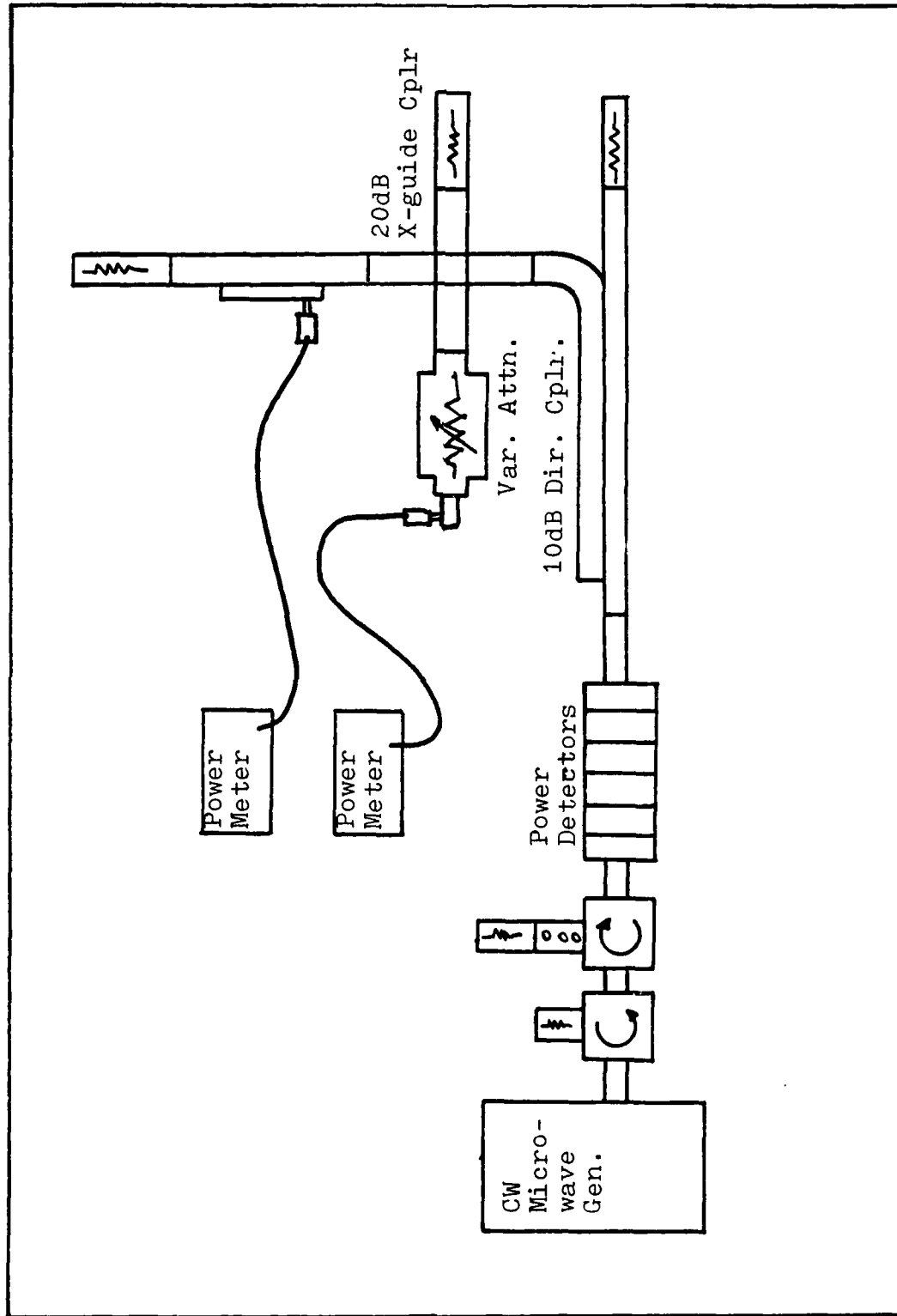


Figure 15. Power Meter Calibration

the directivity of the couplers. Poor directivity would have caused the detector to register power regardless of the direction of the power flow.

A millivolt supply was constructed using a battery to determine the power meter response to the detector voltage output. This data provided a comparison of the digital voltmeter readings to the analog meter indications.

Power-Up, Power-Down

The power-up and power-down procedures were the same for all microwave operations regardless of the discharge tube used. Slight deviations could be tolerated when their effects were taken into consideration.

Power-Up

1. Turn on the house cooling water.
2. Turn on the heat exchanger.
3. Check the water pressure gauges.
4. Apply rack power to the CW microwave equipment.
5. Check the integrity of the microwave plumbing.
6. Set the gas regulator for 5 psi.
7. Open the flow regulator valve on the vacuum system and purge the system.
8. Turn the pulse microwave generator on standby.
9. Turn on the CW microwave generators.
10. Turn on the test equipment.
11. Regulate the gas flow for the desired pressure.
12. Turn on the radiation warning signs.
13. Turn on the high voltage for the CW generators and set the magnetron current.

14. Initiate the discharge, if necessary, with the Tesla Coil.
15. Check or set the microwave power as required.
16. Turn on the high voltage to the pulsed microwave supply.
17. Adjust pulsed microwave pulse parameters.
18. Make the required I-V measurements.

Power-Down (end of day)

1. Turn the pulse microwave generator to standby.
2. Turn the CW magnetron current to zero.
3. Turn the CW generators' high voltage off.
4. Shut off the gas flow.
5. Turn off the radiation warning light.
6. Shut down the CW generators.
7. Disconnect the rack power for the CW generators.
8. Turn off the pulse microwave source.
9. Turn off all test equipment.
10. Turn off the heat exchanger.
11. Shut off the house water.
12. Recheck all power.

Between experimental runs, the microwave energy was shut down and the gas system would be purged after a cylinder was changed.

IV-C for Discharge Tube I

Current voltage characteristics, IV-C, for the first discharge geometry were recorded on an X-Y recorder. The X-axis was driven by the voltage that was placed across the

discharge tube and the current monitor resistor. An attempt was made to float the input to the X-axis channel off of ground so that the X position would be equivalent to the voltage applied to the discharge tube. This would not work due to the relatively low input impedance of the X-axis channel. The generator output was loaded down and the current through the monitor resistor had a large component contributed by the X-axis plugin. Also, with the ground floating, there was a considerable noise component which was reduced once the input was grounded.

The current through the discharge was monitored as the voltage across a series resistance. This voltage was applied to the Y-axis input.

Both channels experienced a lot of noise so the recorder was operated with the set-up mode filter to reduce the load on the recorder's servo system. When the IV-C was taken for a run, the result was an almost linear plot with a slope that was proportional to the microwave power input. The voltage generator was applying a ± 10 volt triangular wave at a frequency of about 10 cycles per minute to the discharge tube. In this configuration, a loop would form at the tip to the plot when the X-drive would change direction with the applied voltage. It was found that this was due to the lower frequency response of the servo system in the set-up mode. Once this problem was identified, the remaining traces were taken in the record mode.

The gases which were used in the first discharge tube were 10% nitrogen-90% helium mixture and tank helium. The nitrogen-argon mixtures were not used at this time due to their late arrival. Data runs were made at different pressures and microwave powers, Figures 16 and 17. The power meter readings were taken using a rotary switch which would connect a digital voltmeter to all the power detectors. This data was used to compute the actual power going into the discharge.

The final run in the first discharge tube was at 0.5 torr of helium with about 500 watts of CW microwave power. The discharge around the electrodes took on a different color. When the microwave power was shut down, it was observed that the aluminum electrodes had experienced unexpected heating producing surface melting and warping. Subsequent tests with aluminum in the microwave fields at atmospheric pressure without a temperature rise indicated that the electrodes had not been heated by ohmic heating with surface currents from the microwaves. It was concluded that the damage was due to plasma heating and radiation.

IV-C for Discharge Tube II

With the second discharge tube the electrodes were separated by 40.5 centimeters. In order to achieve the same range of E/N that was used for the first tube, it was necessary to use a higher voltage source. A DC supply (HP 212B) was used and the voltage was controlled by hand.

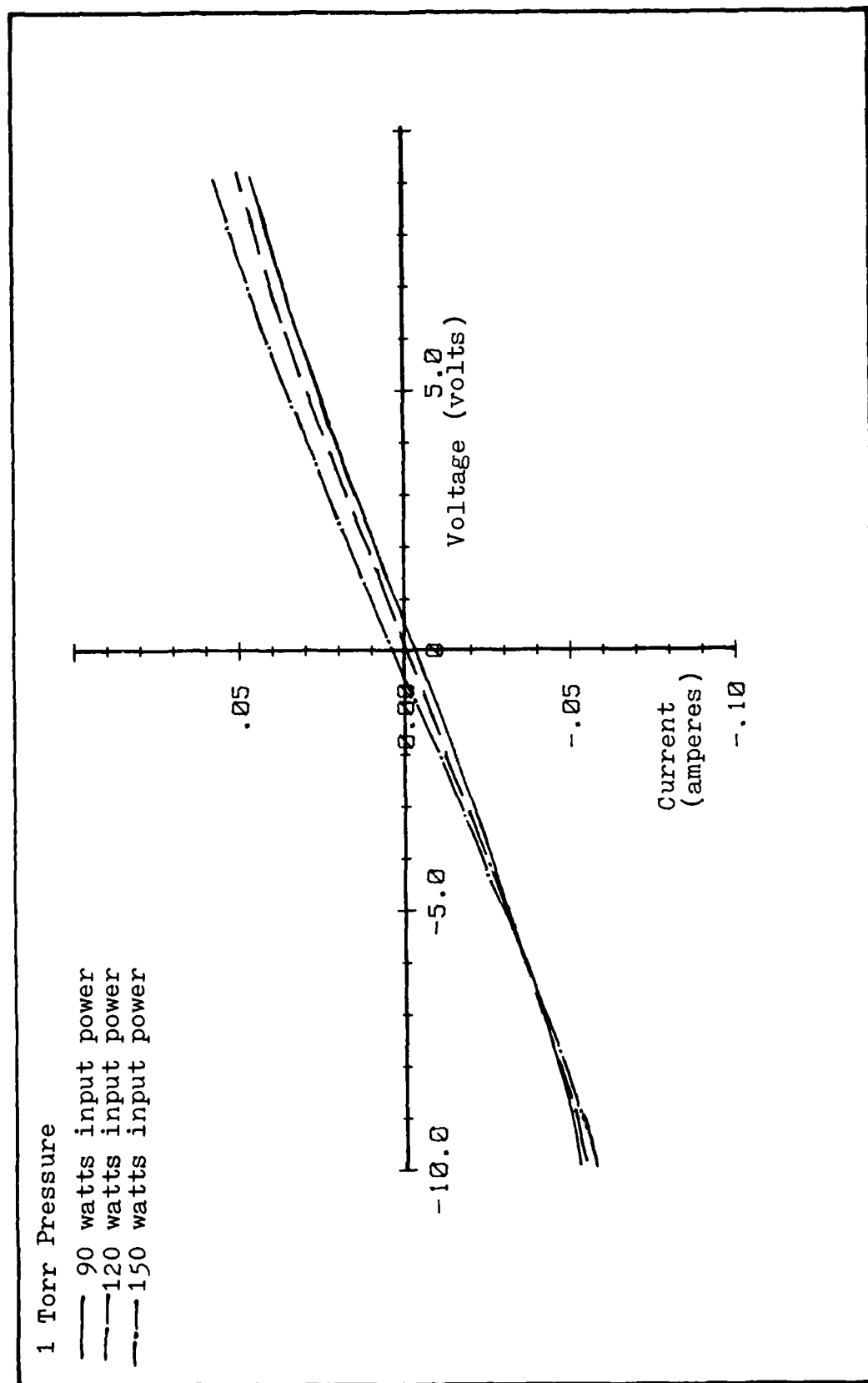
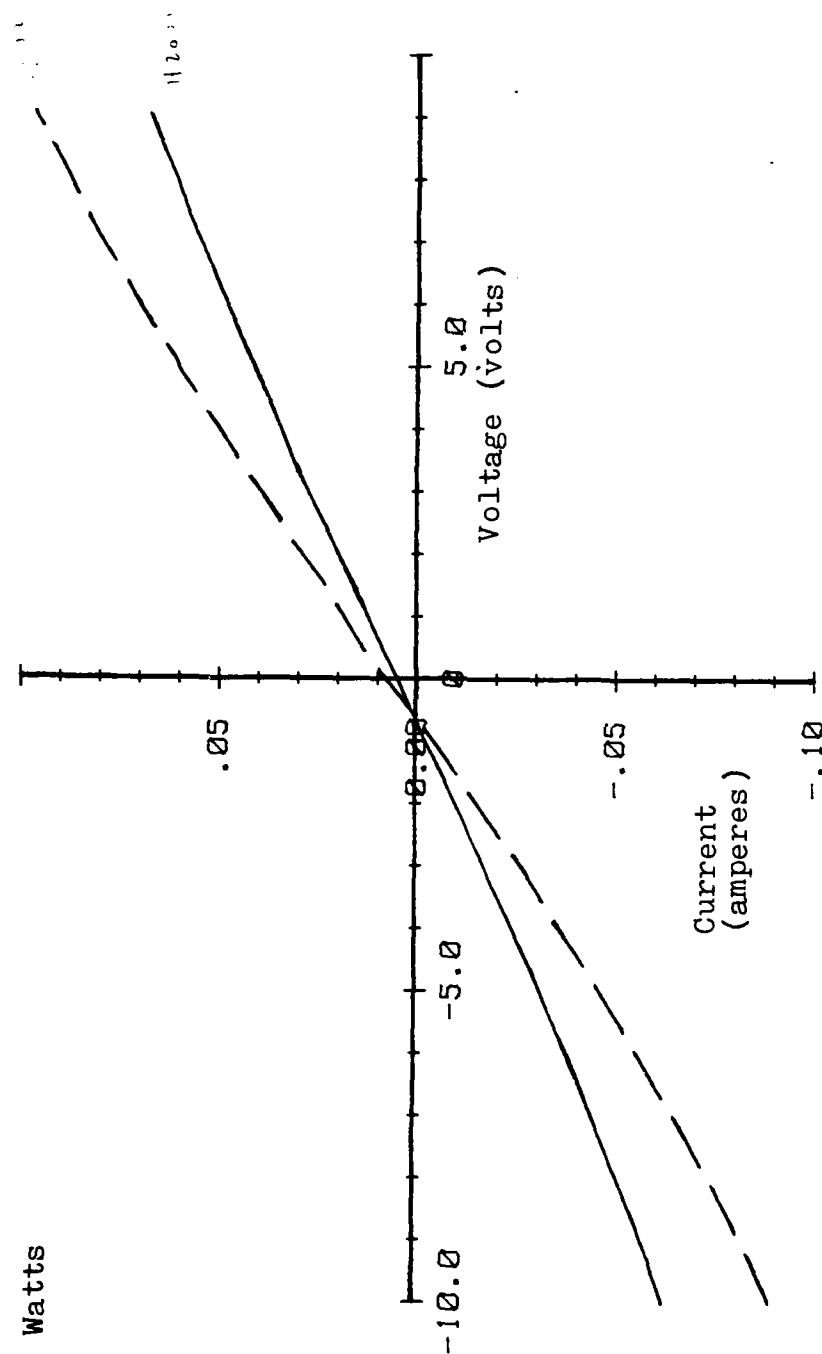


Figure 16. I-V Characteristics for 10% Nitrogen in Helium in Discharge Tube I

0.5 Torr Pressure
150 Watts



Note. The dashed curve was taken about ten minutes after the other.
The discharge was always on.

Figure 17. I-V Characteristics for 100% Helium in Discharge Tube I

The X-Y recorder connections remained the same. To use the entire voltage available from the power supply (500V), it was necessary to reduce the sensitivity of the X-axis input channel. When the sensitivity was reduced, a scale was placed on the plot to indicate the X voltage scale. Calibration marks were made by making a separate trace and marking 25 or 50 volt increments as measured on a Fluke digital multimeter (see Figure 18).

The gases used in making these plots were 9.82% nitrogen in argon and 10% nitrogen in helium. The apparent saturation in the IV-C was unexpected. A switch was installed that would allow reversal of the cathode-anode connections. Under the same conditions, but with the cathode and anode positions reversed (electrically), the trace had a slightly lower saturation value.

As the voltage was increased beyond the point of apparent saturation, there was a slight jump in the current followed at a higher voltage by a steady increase in current with increasing voltage. With the aid of other observers it was found that the 'jump' in current as the voltage was increased occurred at the same time as a sudden increase in cathode involvement; that is, the glow discharge suddenly extended itself over more of the cathode (about one square centimeter). As the voltage was decreased from its highest level, another 'jump' in current occurred, decreasing the current suddenly. This sudden

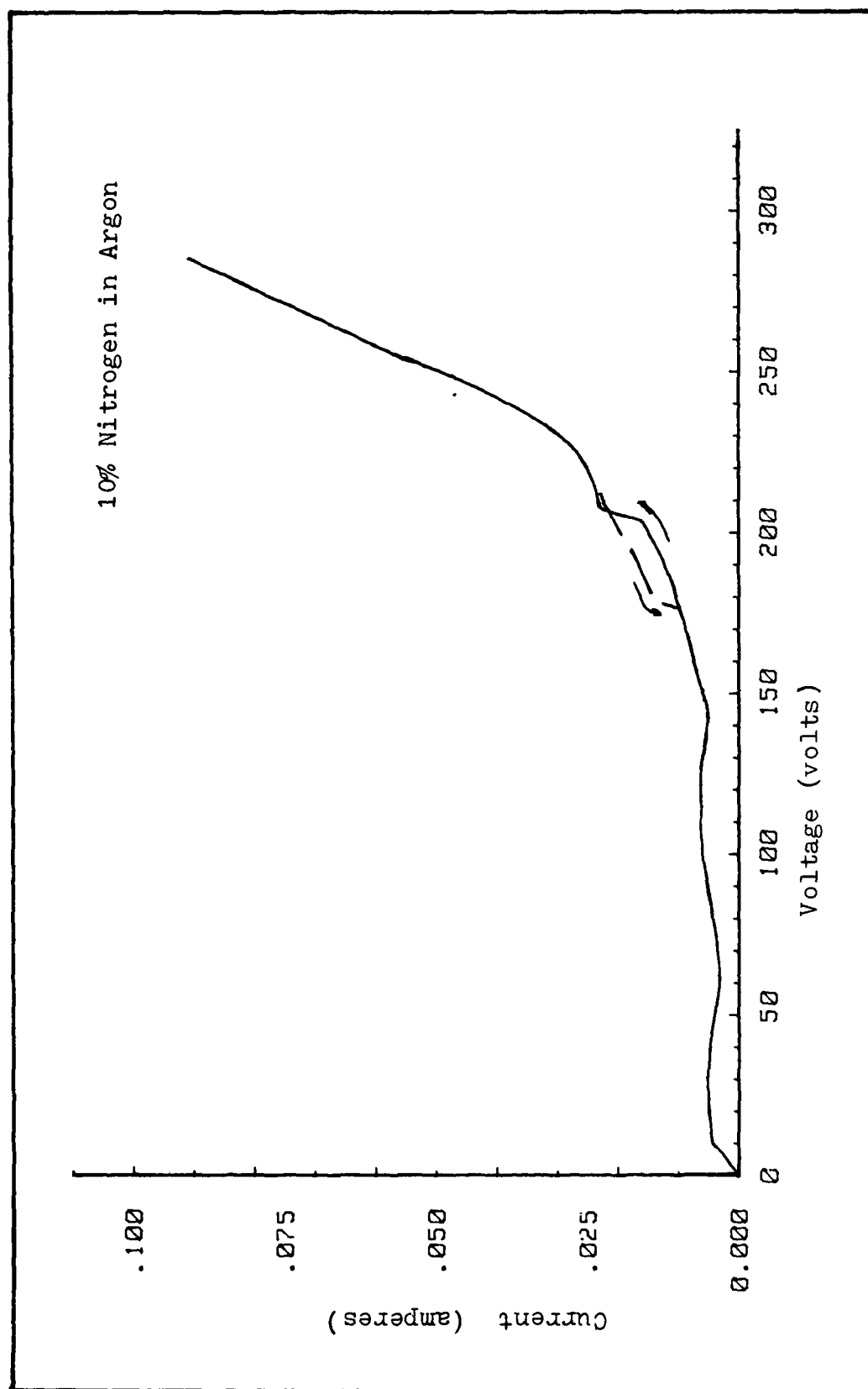


Figure 18. DC Characteristics for Tube II

decrease in current occurred at a lower voltage than the sudden increase and was coincident with a decrease in cathode involvement.

It was speculated that the increase in current after the saturation region with increasing voltage was due to the onset of Townsend ionization and possibly a DC sustained discharge. To check this, the microwaves were interrupted in this region (275 volts with 100ma current). The discharge current dropped to zero and the discharge was extinguished. While Townsend ionization may have begun, it was not adequate to sustain the discharge.

In an effort to get away from effects which may happen on the order of a diffusion (radial) time constant (about 160 microseconds) or longer, leading to saturation, the IV-C was made using a pulse generator and an oscilloscope monitor. A General Radio pulse generator with a variable pulse length was used to supply the 'DC voltage'. The pulse width was long compared to the microwave period and the time it takes the discharge to reach steady state current. The discharge current and voltage waveforms were observed on a dual channel Tektronix 556 oscilloscope.

During the initial attempts at pulsed operation a considerable amount of noise and gross fluctuation appeared on the pulsed current traces. Two types of noise were identified and it was possible to eliminate their effects. There was a 360 Hertz ripple noise component which was due to line frequency ripple (three phase-full wave

rectification) in the high voltage supply for the magnetrons. These variations in the high voltage caused corresponding fluctuations in the microwave power output. The effects of this noise were avoided by synchronizing the pulse measurements on the line voltage and making the pulse much shorter in time than the variation due to the ripple.

Another noise source was the coupling of microwave power to the oscilloscope through the current monitor leads. The effects of this were reduced using a Tektronix 1A7A plugin with a 1MHz lowpass filter.

For the pulse measurements, about 140 watts of microwave power (as read on the input meters) was used to sustain the discharge. The reflected and transmitted power will be taken into account in the analysis. A pulse width of 5 microseconds was applied at various voltages and the corresponding amplitude of the current waveform was measured. The current waveform amplitude was recorded at 0.4 and 4.0 microseconds after the beginning of the pulse for the argon and argon-nitrogen gases. The helium and helium-nitrogen gases were measured at the 4 microsecond point.

Recording the current pulse amplitude at 0.4 microseconds was prompted by the fact that the argon and argon-nitrogen gases would show a peak at the beginning of the pulse at input voltages greater than 8 to 10 volts, regardless of the pressure. After the peak at the leading

edge of the pulse, the current would drop to a constant value until the end of the pulse. Variation in the width of the applied pulse did not change the current waveshape behavior.

As the voltage pulse was increased in amplitude, the discharge current began to load the generator output. Care was taken to read the voltage pulse at the same points in time as the current waveform. The results of the pulse IV-C readings at 0.4 and 4.0 microsecond points can be seen in the appendix.

It was found that when the current had reached its saturation value, it could be increased by increasing the microwave power to the discharge. While the discharge current would increase, it would still reach a saturation point with increasing voltage, for a given microwave power input.

In an attempt to determine, qualitatively, if the saturation effects observed were cathode sheath dominated, a permanent magnet was inserted in the cathode region (outside the tube) while observing its effects on the discharge current. Observations were made with the input pulse at a voltage below saturation and at a level above saturation. It appeared that the magnet's presence produced a greater percentage effect at the saturation level. When the magnet was placed near the anode, the results were not as dramatic.

Another approach to perturb the cathode sheath effects was to use the microwave pulse generator and feed in to the cathode area a 2 or 3 kilowatt pulse. This should create a

local increase in ionization and generate ultraviolet radiation which would produce photoelectrons at the cathode. The pulsed microwave source was triggered by the A-channel delayed gate output from the oscilloscope. This allowed movement of the pulse in time to points before, during, or after the voltage pulse. Introduction of the microwave pulse during or before the voltage pulse resulted in a large increase in discharge current. There would be an increase in discharge current even if the microwave pulse had completed its pulse prior to the voltage pulse turn-on. The fact that the current increase occurred even after the microwave pulse was turned off indicated that direct ultraviolet initiated emission of electrons from the cathode was not the cause but rather a buildup of electron density in the sheath. If the microwave pulse ended within the voltage pulse time frame, the current would quickly return to its 'DC only' level.

The observations made with the magnet and microwave pulse were only qualitative. Their purpose was to help satisfy the assumption that the observed IV-C were cathode sheath dominated.

MD-A135 651

DISCHARGE UNDER THE COMBINED INFLUENCE OF DC AND RF
FIELDS(U) AIR FORCE INST OF TECH WRIGHT-PATTERSON AFB
OH SCHOOL OF ENGINEERING J A THORNE DEC 82

2/2

UNCLASSIFIED

AFIT/GE0/PH/82D-14

F/G 20/3

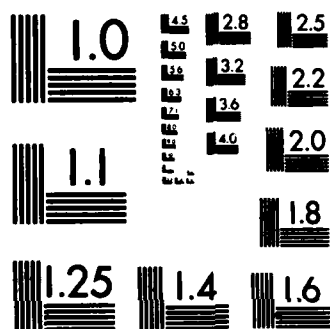
NL

END

FILMED

1-84

DTIC



MICROCOPY RESOLUTION TEST CHART
NATIONAL BUREAU OF STANDARDS-1963-A

V. Analysis and Conclusion

The purpose of this section is to analyze the data taken in terms of the two models presented in the theory section. Also, the assumptions that were outlined in Model I will be examined. The analysis will be divided into three parts which will look at the three basic kinds of data taken. First, the data taken with the first discharge tube will be analyzed. Second, the DC measurements in the longitudinal discharge tube will be considered. Finally, the pulsed measurements will be examined. Conclusions that were drawn are presented in each of these sections where appropriate, with general concluding remarks at the end.

The sequence of analysis follows that of the actual experimental work and, in that sense, follows the evolution of the thinking and understanding of the problem. In addition, in this section, license will be taken to mention qualitative observations that may support conclusions drawn in the analysis or be of value in future analysis or experimental work. This section does not attempt to completely exercise the theory of Model II or test its validity.

Initial Data, He and He-N

The data taken in the first discharge tube with 100% helium and 10% nitrogen in helium was intended to be

preliminary only and to test the apparatus. However, even though the cathodes melted prior to use with the argon-nitrogen mixtures, there is still some valuable information in the I-V characteristics that were taken.

From the I-V characteristics for 10% nitrogen in helium, Figure 16, a definite increase in slope is observed with increasing microwave power. The volume between the electrodes of the discharge is analogous to an ionization chamber in which the amount radiation is measured by the current produced when the ion-electron pairs are swept out by the application of a DC potential. In this experiment, the microwaves are providing ion-electron pairs between the electrodes and the measured current is proportional to the quantity of carriers available for conduction. The current for this set of curves follows equation (37) from Model I

$$I = n_e e W A \quad (77)$$

In order to test the model, established values of drift velocity were used to calculate the electron number density from the current. The area of the electrodes was approximated to be 21.2 cm². Values of drift velocity W for electrons in 10% nitrogen in helium were supplied by Garscadden (Ref 16). Using these values, it was found that the electron density was approximately 1×10^{10} cm⁻³ and increased slightly with E/N. This slight increase

in density with E/N was about 1×10^{10} in one Td. This was not expected and may have been due to way the higher values of drift velocity were extrapolated from the theoretical values supplied. The relative magnitude of the electron density was about that expected. Electron densities of about 10^{10} had been previously reported for similar microwave discharges (Ref 24).

The zero current cross-over point on the voltage axis (Figure 16) was constructed. The data for this curve was taken without a zero current (discharge off) reference. Later data taken shows that the vertical axis should fall to the right of the zero cross-over points for all of the curves in Figure 16 as it does in Figure 17. Figure 17 shows two I-V curves taken at the same power but separated in time. The zero cross-over here occurs at the same point. This shift left (to negative voltages) for the zero cross-over is believed to be due to the effects of field asymmetry due to the presence of the (near) grounded electrode in the discharge combined with diode action of the cathode sheath.

This bias current would be proportional to the electric field strength and thus to the amount of input power.

The increase in conductivity shown in Figure 17 is probably due to the increased plasma temperature.

Temperature measurements taken with a thermometer against the outside of the discharge tube near the electrodes had shown temperature rises of 20 to 30 degrees centigrade. Besides having a hotter plasma, this would translate into a decrease in the total number density within the discharge tube, raising the E/N .

DC Characteristics in the Longitudinal Tube

In a microwave discharge, ionization is supplied by the microwave field interaction with the free electrons. As long as the discharge is uniform and there are sufficient electrons generated throughout the volume, Model I predicts that a current will follow the drift velocity increase with E/N . At high values of E/N , electrons may be swept out of a region before they can participate in ionization. The region of the cold cathode (which does not produce electrons) can become void of electrons and thus fail to generate additional electron-ion pairs. Instead of a neutral plasma throughout the volume, a region around the cathode called the cathode sheath develops with only positive charges (ions), Figure 4.

In this thin cathode sheath the production of ion-electron pairs occurs near the edge of the positive column. The current in the cathode sheath then is accomplished by the electrons and ions near the positive column boundary but reduces to only positive ion current near the cathode as the electron density drops to near zero.

The sheath development can be seen in the current-voltage characteristics where the initial slope (electron dominated) begins to decrease to almost horizontal (positive ion dominated in the sheath) (see the four microsecond pulse measurements in the appendix). The transition between the two reflects the decreasing role of the electrons as current carriers in the sheath as this role is taken over by the positive ions.

As the DC voltage is increased across the electrodes, cathode sheath limiting occurs at about 10 to 15 volts for the mixture of 10% N-He at 4 torr (Figure 18). An increase in voltage shows no corresponding increase in current until the voltage is about 175 volts. In this region a visible increase in cathode surface involvement was observed causing a 'jump' in the current. Also, in this region (of voltage) the electric field in the cathode region is becoming sufficient to cause Townsend ionization. Townsend ionization within the cathode sheath results in a dramatic increase in the positive ion density and corresponding increase in the discharge current. The slope of the I-V characteristic increases accordingly.

To estimate the electric field strength in this region, equation (66) is used to calculate the cathode sheath thickness. Equation (67) is substituted in for $e v_{ie} n_0 \Lambda$, then,

$$V_c = \left(\frac{8eV_i m_e A}{9\epsilon\mu} \right)^{1/2} b^{3/2} \quad (78)$$

$$V_c = \left(\frac{8 I_{sat}}{9\epsilon\mu A} \right)^{1/2} b^{3/2} \quad (79)$$

Substituting the current at saturation for I, 1470 for μ , and the cathode surface area for A.

$$V_c = \left(\frac{8(7.5 \times 10^{-3})}{9(8.85 \times 10^{-14})(1470)(20)} \right)^{1/2} b^{3/2} \quad (80)$$

or

$$b = \left(\frac{1}{2.56 \times 10^2} \right)^{2/3} V^{2/3} \quad (81)$$

For values of V_c , the voltage where I becomes saturated is subtracted from $V_{applied}$. Looking then at 175V, this becomes $175 - 15 = V_c$ and b becomes

$$b = (3.9 \times 10^{-7})^{1/3} (160)^{2/3} = 0.215 \text{ cm} \quad (82)$$

and the electric field is

$$E_c = \frac{V_c}{b} = \frac{160 \text{ V}}{0.215 \text{ cm}} = 743 \text{ V/cm} \quad (83)$$

Using this value of electric field in Townsend's equation for α

$$\frac{\alpha}{p} = A \exp \left[-\frac{B}{(E/p)} \right] \quad (84)$$

A and B are empirically determined constants where

A = 13.6 and B = 235 (Ref 25:149), this becomes

$$\alpha = 4(13.6) \exp \left[-\frac{2.83(235)}{635} \right] \quad (85)$$

$$\alpha = 19.1 \text{ cm}^{-1} \quad (86)$$

As the values of E/N approaches (2.83*235) the α term becomes significant and ionization is increased in the cathode sheath region, adding to the current conduction. This accounts for the sharp rise in current around 175 volts in Figure 18.

Saturation was experienced for this tube for an E/N on the order of about 0.3 to 0.4 Td. This is considerably lower than the E/N's experienced in discharge tube I where saturation effects were not observed. The difference probably has to do with the type of cathode used in the second tube. The actual cathode surface is not well defined for this tube. Ionization was observed within the cathode cylinder and this was assumed to be the primary cathode surface. In this region, however, the microwave intensity was probably considerably reduced.

This would account for the cathode sheath formation at the lower E/N.

Pulse Characteristics

The saturation limiting due to the cathode sheath effects were also observed in the pulsed measurements. In addition to the saturation effects with increasing DC voltage applied to the discharge, there was a peak at the leading edge of the current pulse. This peak at the leading edge would appear when the di/dV of the I-V curve began to decrease, indicating the onset of the sheath. The values of the peaks, measured at 0.4 μ sec, were plotted against their corresponding voltage (and E/N); see appendix.

In order to analyze these leading peaks it was assumed that during this time ($< 0.5\mu$ sec) the cathode sheath had time to completely form to its limiting value. Using the theoretical values of drift velocity (Ref 16), the electron number density was calculated from equation (37) from Model I, $I = n_e W e A$. The value of A used was the cross-sectional area of the discharge tube, 2.27 cm^2 . The values of electron density were found to be nearly constant even as the current and drift velocity varied as much as 50 per cent. The electron densities were on the order of $5-11 \times 10^{10} \text{ cm}^{-3}$ for the data runs at one and four torr and from $3-5 \times 10^{10} \text{ cm}^{-3}$ at 0.5 torr. These

densities were in line with those found earlier in discharge tube I.

When the power meters were read, it was found that there were measurable amounts of reflected power (5-15 watts) for the argon, 1%N-A, and 0.1%N-A gas mixtures only. From the conditions for reflection (Ref 17:141), "the electron density to which, at normal incidence radiation of $f = \omega/2\pi$ penetrates before reflection" can be found from

$$n_e = \frac{m \epsilon_0 \omega^2}{e^2} \quad (87)$$

(Ref 16:141)

$$n_e = \frac{9.1 \times 10^{-31} (8.85 \times 10^{-12}) (1.6 \times 10^{10})^2}{(1.6 \times 10^{-19})^2} = 8 \times 10^{16} \text{ m}^{-3} \quad (88)$$

$$= 8 \times 10^{10} \text{ cm}^{-3}$$

These values were exceeded by the argon and argon-nitrogen mixtures (1 and 0.1%) at both one and four torr. However, the 9.82%N-A mixture (which gave no measurable reflections) had a density of only around $5 \times 10^{10} \text{ cm}^{-3}$.

The values of electron density calculated from the current peaks also show a slight decrease (about 10% per Td) with increasing E/N. This could possibly be due to a more rapid sheath formation with high E/N, assuming the theoretical values of drift velocity are accurate. The exact leading edge of the pulse could not be determined with accuracy due to noise, so the measurements

at times less than 0.4 μ sec into the pulse would not have been reliable. If this had not been the case, it may have been possible to measure nearer the leading edge. It is not known if this would have shown a more constant electron density.

The I-V characteristic for 0.1% N-A mixture at four torr was analyzed in the saturation region. The electron density was assumed to be constant at 1.43×10^{11} , the value that was calculated from the pulse peak. The drift velocity calculated for this density was $4.2 - 4.39 \times 10^5$. The reduced electric field was approximated from Figure 1 to be about 0.4Td which translates to a voltage of 18 volts. Since the current used in this calculation corresponded to a voltage of 41.5v, approximately 23 volts had to be dropped in the cathode sheath region. This shows that as the applied voltage is increased beyond the saturation point, there is an increase in voltage drop across the cathode sheath with a subsequent increase in the electric fields there.

Conclusions

The uniform plasma and negligible sheath effects assumed for Model I were clearly not met in discharge tube II. Whether they would have been in tube I has not clearly been determined. The asymmetry of the I-V characteristic curve may, however, point to the formation of

a sheath but its fully developed effects were not observed. The requirement that the mean free path be smaller than the plasma dimensions is clearly met in tube II, unless the comparison is made to the cathode sheath thickness. For this case to be analyzed it would be necessary to more clearly define the cathode sheath and develop a way of measuring it. The electron production rate is always greater than the loss due to conduction with the exception of the cathode region. Implicit in the development of the cathode sheath is that the external ionizing source loses its production capability near the cathode due to the loss of the free electrons required by microwave excitation.

The saturation predicted in Model II for a cathode sheath dominated discharge was observed. The author was not able, however, to use the model for any deeper analysis and predictions.

The pulse measurements may provide the drift velocity dependence on E/N for a microwave discharge providing the measurement time is short enough that the cathode sheath has not been fully developed. This should be approached with caution, however, since the sheath formation time may be related to the use of the hollow cathode, long positive column, or some other unpredictable coincidence.

It is clear that the microwave discharge will provide a volume discharge that may see possible application in pulse power switches. The ionization dependence on free

electrons implies that there will always be sheath effects with cold cathode configurations. This may be circumvented by a hot cathode, but it may not require the same kind of emission rates that would be necessary in a tube without microwave excitation.

This experiment certainly does not rule out the possibility of using the microwave sustained discharge to search out parameter ranges for gases which would be more difficult on a more complicated apparatus. It does point out that the discharge has some effects which must be taken into account such as cathode sheath effects, plasma heating, and the asymmetrical field problems. This experiment is merely a short step in that direction.

VI. Recommendations

Recommendations for future work in this area can follow at least two directions. One is that of circumventing the cathode sheath effects of the cold cathode discharge in order to get at the relationship of the drift velocity and E/N . This would probably be most easily accomplished by using a hot cathode supply for the conduction/production electrons. The other possibility is to investigate the cathode sheath effects more completely for the microwave sustained discharge. This could include a more complete theoretical analysis and a computer model.

In order to repeat or extend this study, an independent measurement of the electron density, perhaps spatially and temporally, would be of great help in the analysis. To gain a better grasp of the effects at higher E/N would require a higher power (voltage) generator with a low internal impedance. The wave shape of the generator should be considered for an idealized square pulse that would allow more careful examination of the sheath formation process occurring at the beginning of the pulse and events immediately following the turn off of the pulse.

The injection of a microwave pulse in the cathode region during the pulsed current measurements gave interesting results. Again, sharp rise and fall characteristics would enable measurements of some important

processes such as recombination. The power going into ionization is important and accurate power monitors, sensitive in the operating range (power), are necessary. It is also recommended that pulsed measurements be considered if the microwave power fluctuates with power supply or line frequency ripple.

With the possibility of temperature of the plasma or electrodes playing a role in the observations, some means of monitoring temperature should be used. A cathode with a better defined surface area should be used. And, finally, the effects of field asymmetry due to near ground electrodes must be considered or eliminated.

Bibliography

1. "Technology Offset Solution to High-Voltage Switching," Aviation Week and Space Technology, 114:70 (May 25, 1981).
2. Kristiansen, M., K. Schoenbach (Co-Chairmen), Workshop on Repetitive Opening Switches, January 28-30, 1981, DTIC No. AD A110770 (April, 1981).
3. Dzimianski, J. W., and L. R. Kline. "High Voltage Switch Using Externally Ionized Plasmas," AFWAL-TR-80-2041 (April 1980).
4. Bletzinger, P. "Electron Beam Switching Experiments in the High Current Gain Regime," 3rd International Pulsed Power Conference, Albuquerque, New Mexico, Paper 5-4, (May 1981).
5. Ward, A. L. "Effect of Space Charge in Cold-Cathode Gas Discharges," Physical Review, 112(6):1852-1857 (1958).
6. Averin, A. P., V. V. Aleksandrov, et al. "Non-Self-Sustained Volume Discharges in Nonelectronegative Gases (Theory and Experiment)," Sov. Phys. Tech. Phys., 26(6):665-669 (June 1981).
7. Zakharov, V. V., et al. "Gas Discharge in Nitrogen with Steady State External Ionization," Sov. Phys. Tech. Phys., 21(9):1074 (Sept 1976).
8. Lowke, J. J., and D. K. Davies, "Properties of Electric Discharges Sustained by a Uniform Source of Ionization," J. Appl. Physics, 48(12):4991-5000 (Dec 1977).
9. Hallada, M. R. "Cathode Sheath Effects in Externally-Ionized Gas Discharges," AFIT MS Thesis, AFIT/GEP/PH/81D-4, (Dec 1981).
10. Yamamoto, K. and T. Okuda. "On the Electrical Discharge in DC and High Frequency Fields Simultaneously," Appl. Sci. Res., B(5):144-147 (1955).
11. Lobov, G. D. and V. V. Zakharov. "Variation of Directional Electron Current in a Gaseous Discharge Acted Upon by a Microwave Field," Radio Engineering and Electronic Physics, 4:614 (April 1962).

12. Nagy, T., L. Nagy, and S. Desi. "Drift Velocities of Electrons in Argon, Nitrogen and Argon Mixtures," Nuclear Inst. and Methods, 8:327-330 (1960).
13. Long, W. H., W. F. Bailey, and A. Garscadden, "Electron Drift Velocities in Molecular-Gas-Rare-Gas Mixtures," Physical Review A, 13:471-475 (Jan 1976).
14. Christophorou, L. G., et al. "Gases for Possible Use in Diffuse Discharge Switches," Advanced copy, Accepted for publication in Applied Physics Letters.
15. MacDonald, A. D. Microwave Breakdown in Gases. New York: John Wiley and Sons, 1966.
16. Garscadden, A. Private Communication (Oct 1982).
17. Howatson, A. M. An Introduction to Gas Discharges, Oxford, England: Pergamon Press Ltd., 1965.
18. Brown, S. C. Basic Data of Plasma Physics, Cambridge, Mass: The M.I.T. Press, (1967).
19. Engel, A von, Ionized Gases, London: Oxford Coventry Press, (1965).
20. Brown, S. C. Introduction to Electrical Discharges in Gases, New York: John Wiley and Sons, (1966).
21. Brown, S. C. "High-Frequency Gas-Discharge Breakdown," Technical Report 301, Research Laboratory of Electronics, MIT, (July 1955).
22. Annette, D. (Thermix, Inc.) Private Correspondence (Aug 1982).
23. Chang, T. Y. "Improved Uniform Field Electrode Profiles for TEA Laser and High-Voltage Applications," Review of Scientific Instruments, 44(4):405-407, (April 1973).
24. Andrews, M. L. "Microwave Plasma Excitation," Progress Report, Technology, Inc., for Aero Propulsion Laboratory (March 1975).
25. Cobine, J. D. Gaseous Conductors, Theory and Engineering Applications, New York: Dover Publications, Inc. (1958).

APPENDIX
Pulsed Current-Voltage Characteristics
for Discharge Tube II

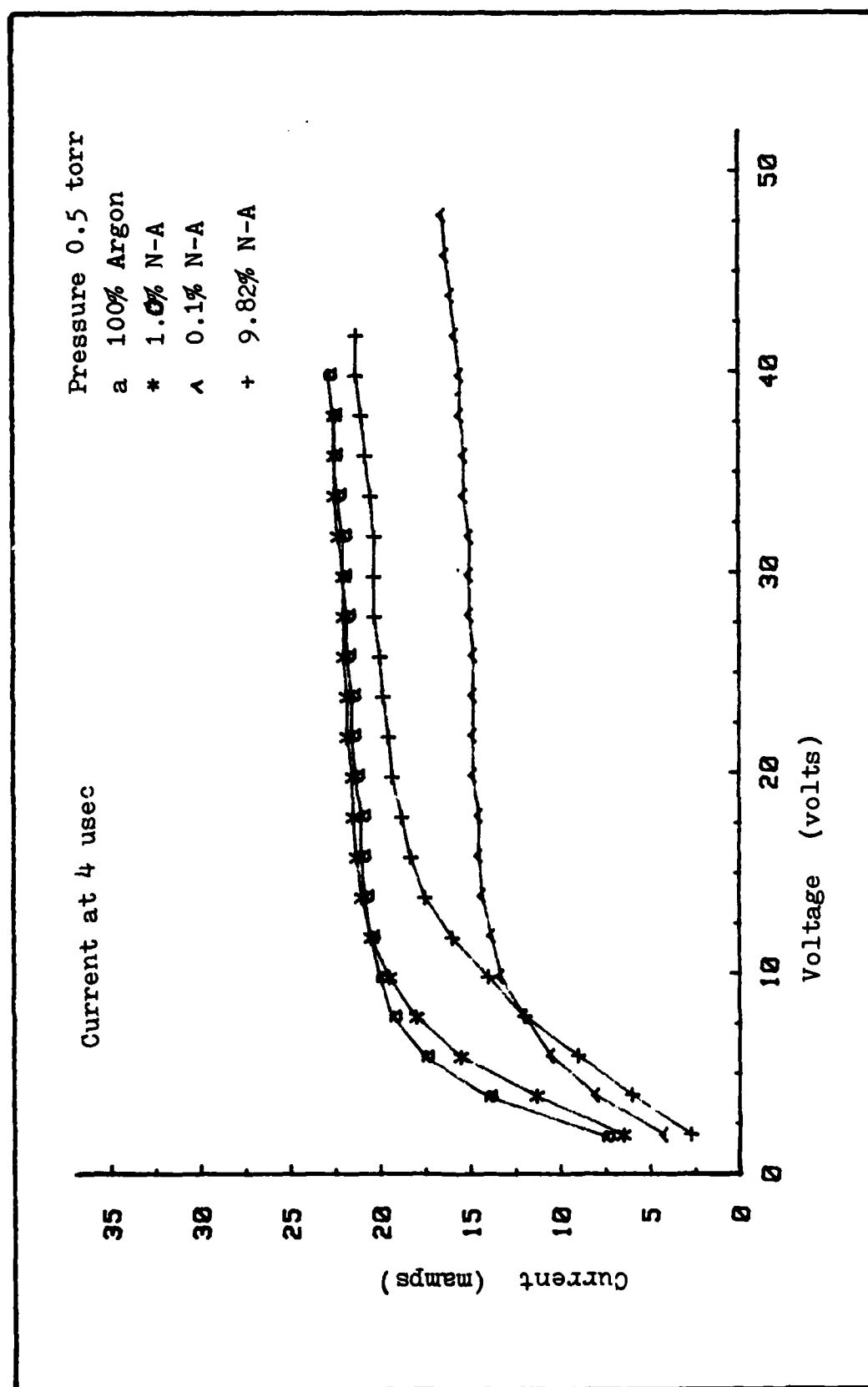


Figure 19. Pulsed I-V Characteristics for Discharge Tube II (0.5 torr)

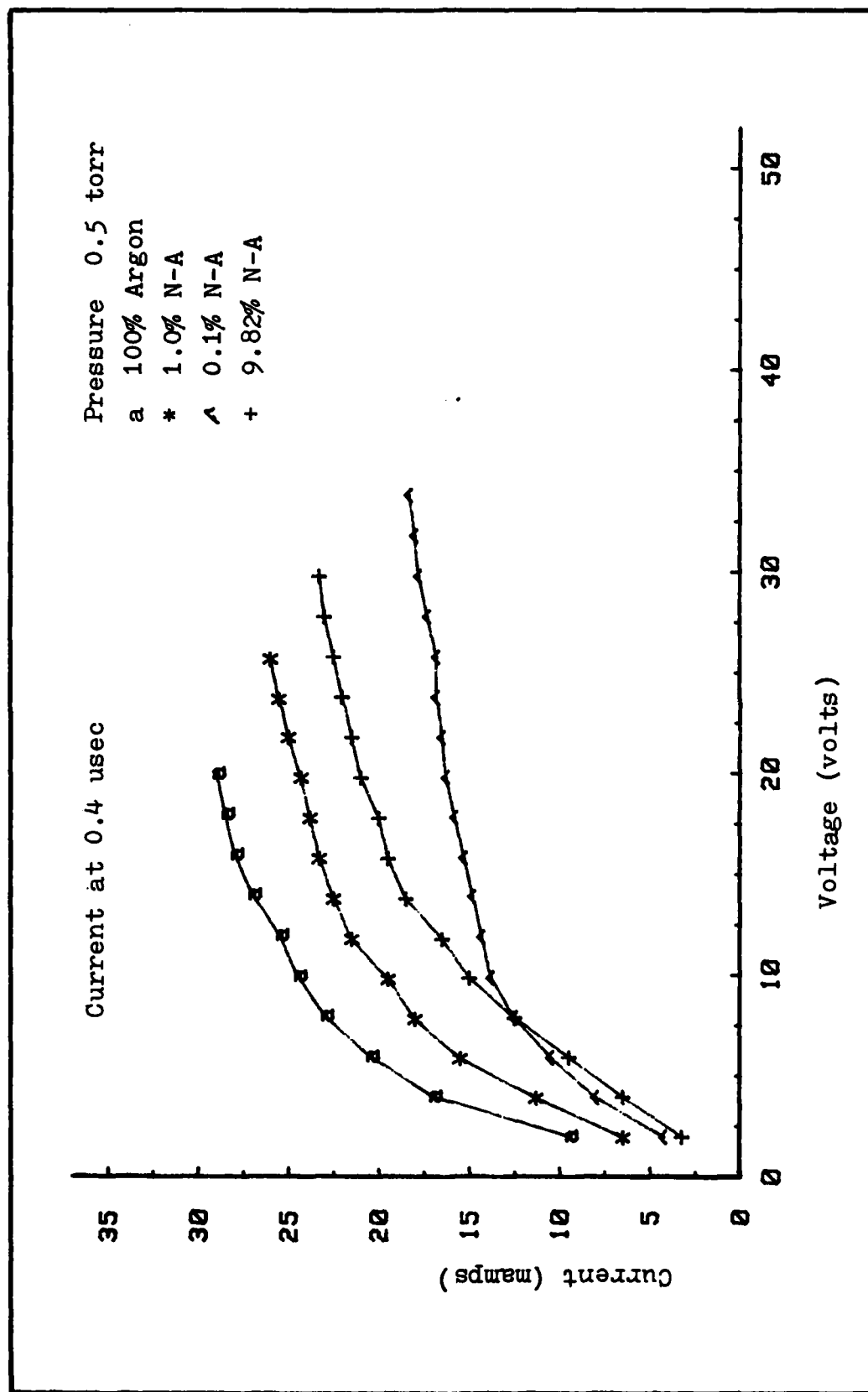


Figure 20. Pulsed I-V Characteristics for Discharge Tube II (0.5 torr)

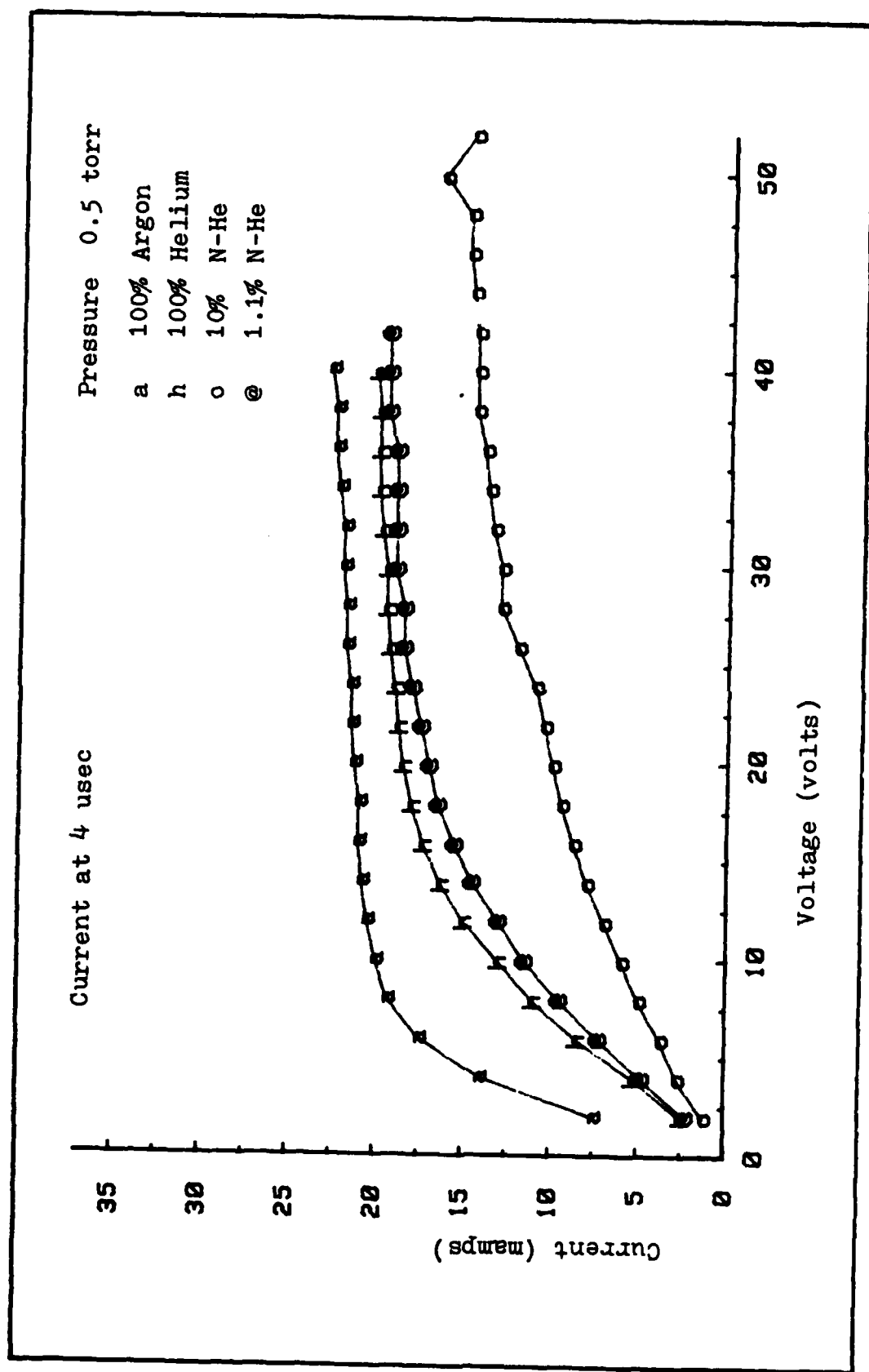


Figure 21. Pulsed I-V Characteristics for Discharge Tube II (0.5 torr)

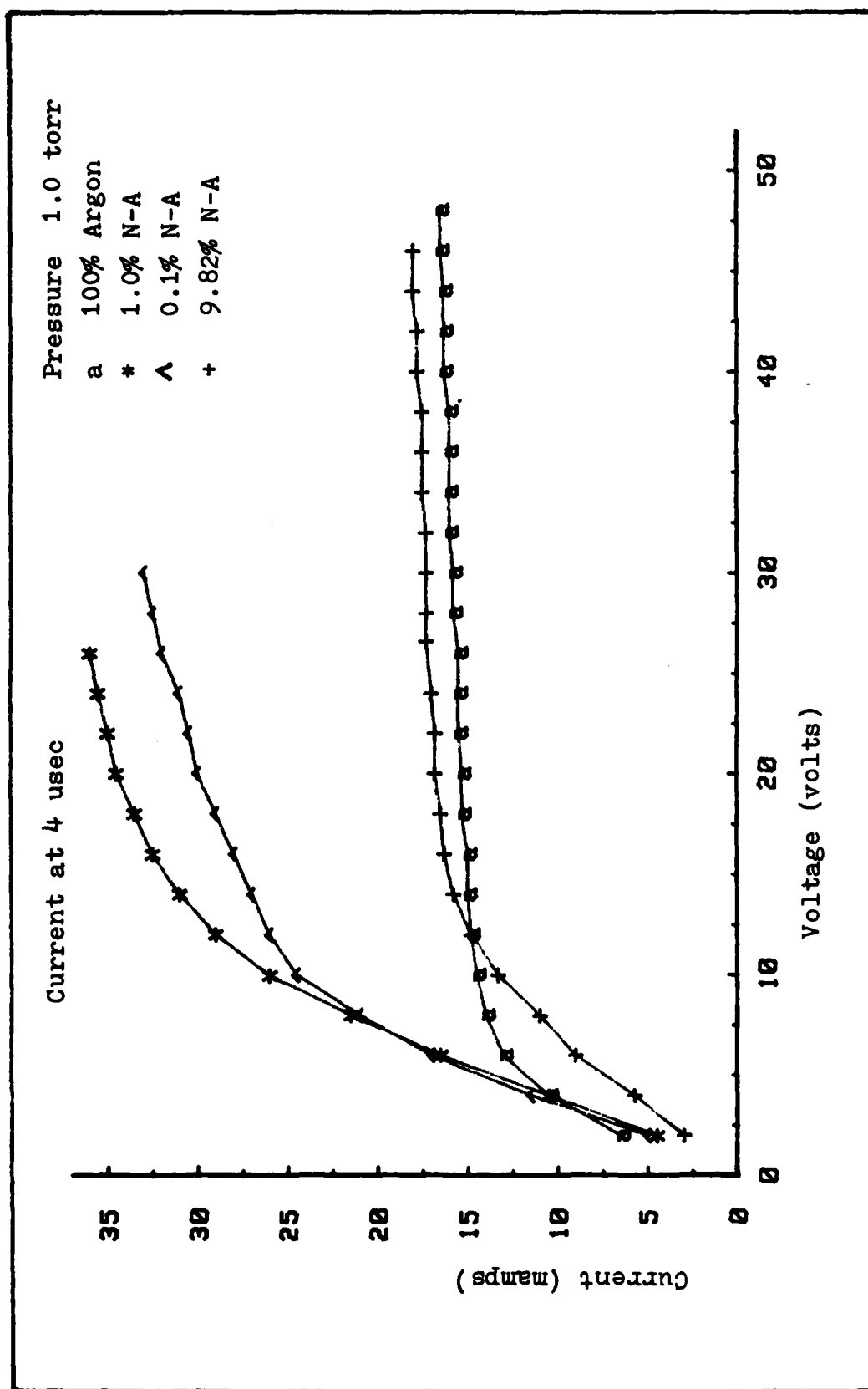


Figure 22. Pulsed I-V Characteristics for Discharge Tube II (1.0torr)

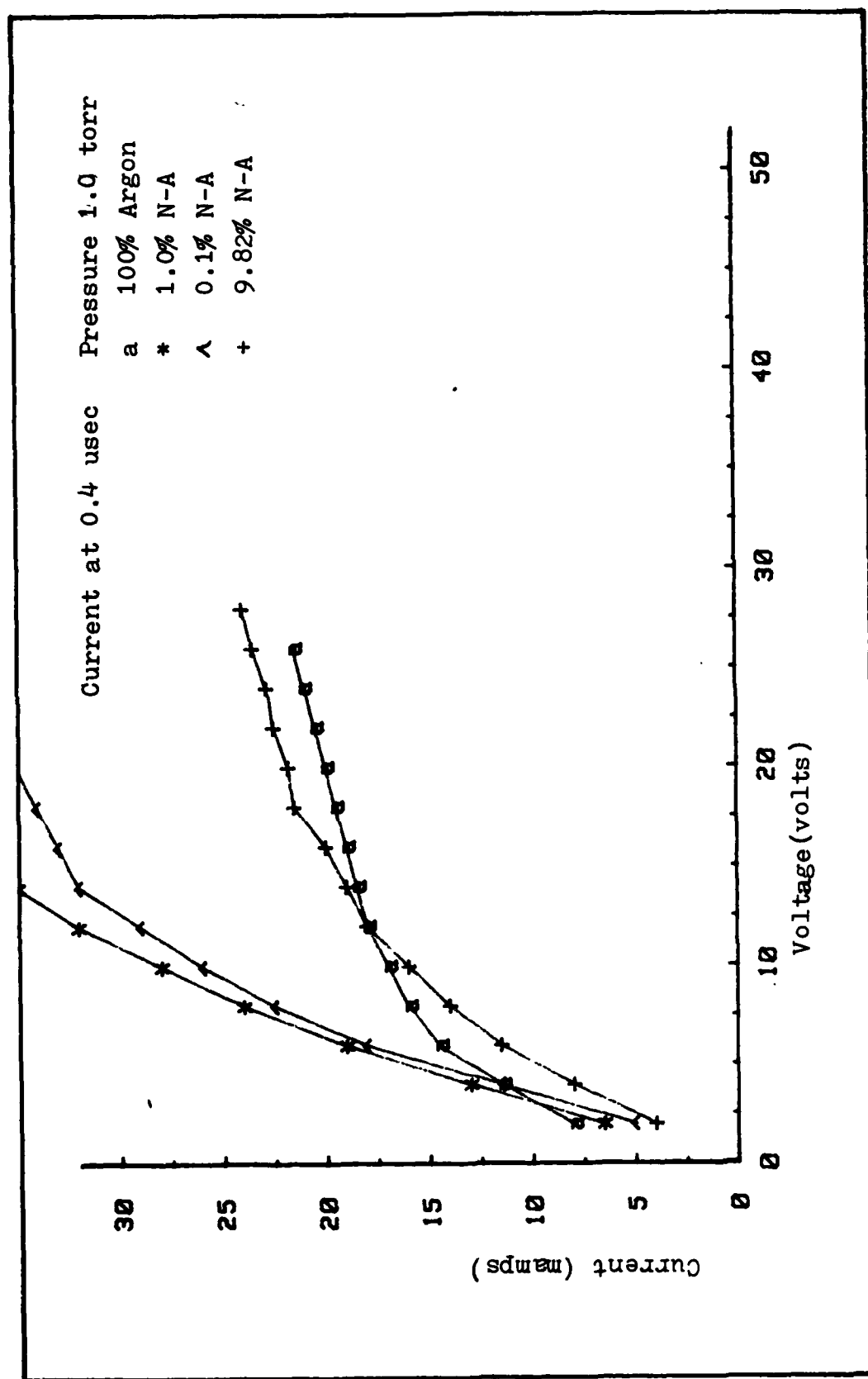


Figure 23. Pulsed I-V Characteristics for Discharge Tube II (1.0 torr)

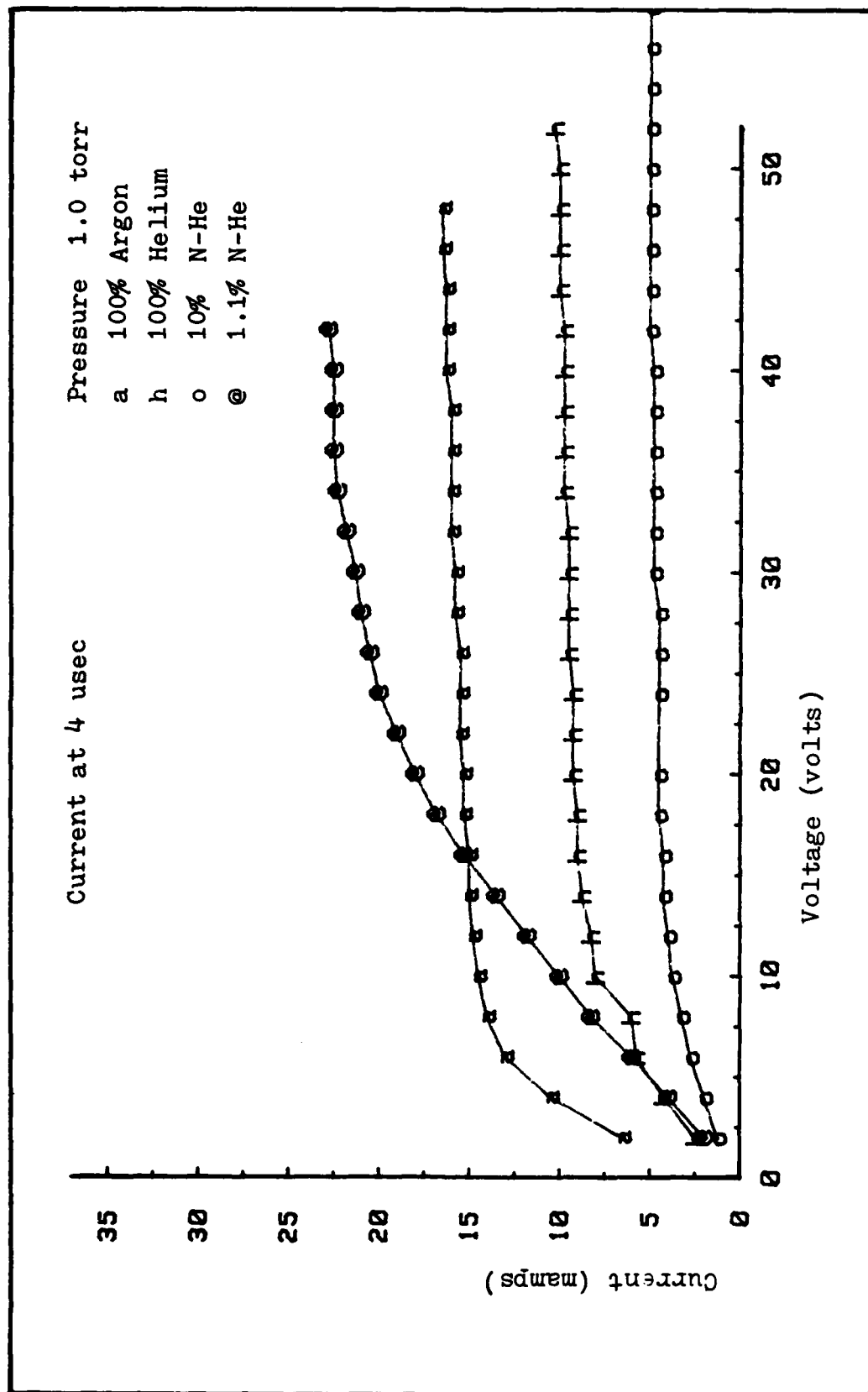


Figure 24. Pulsed I-V Characteristics for Discharge Tube II (1.0 torr)

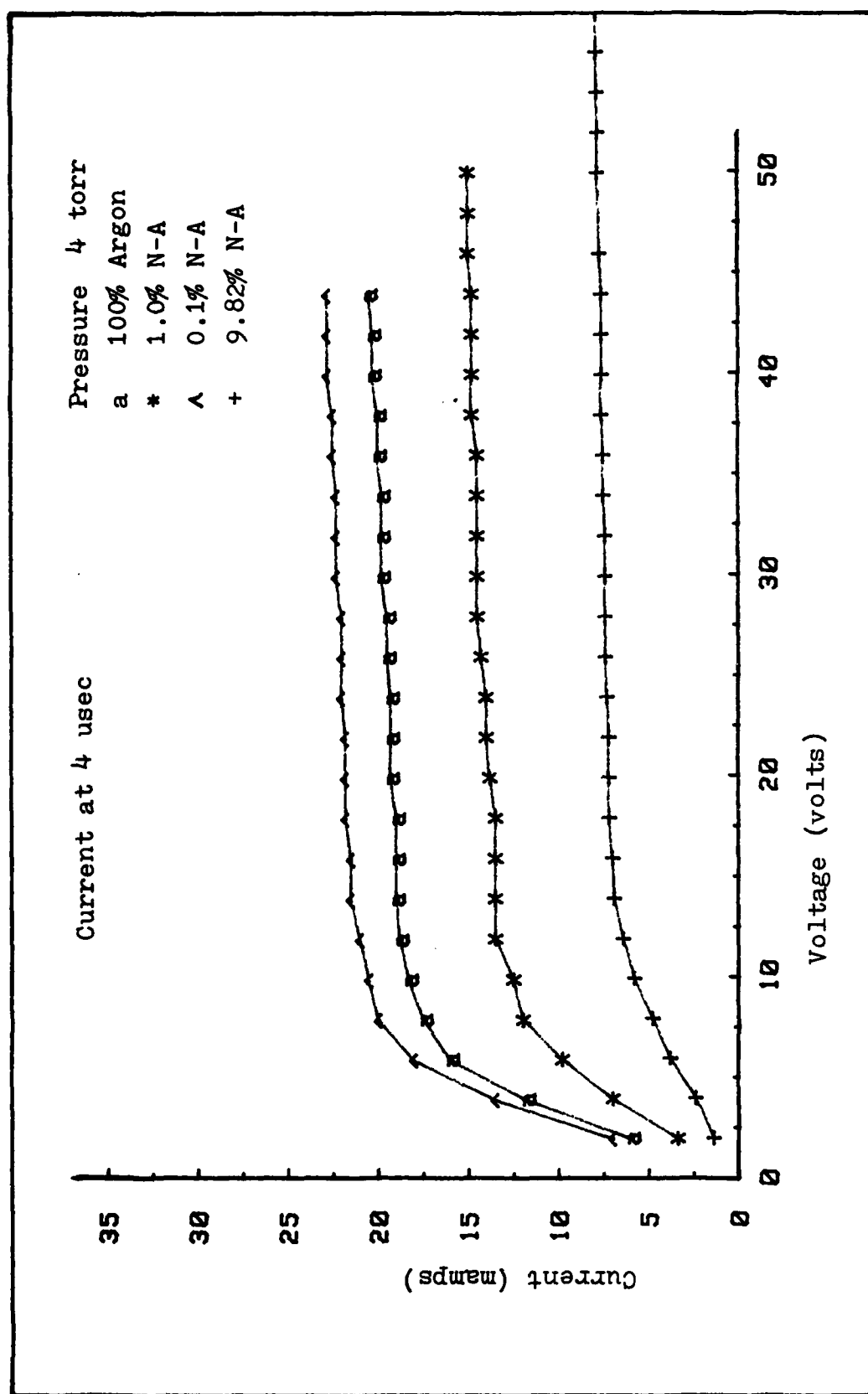


Figure 25. Pulsed I-V Characteristics for Discharge Tube II (4.0 torr)

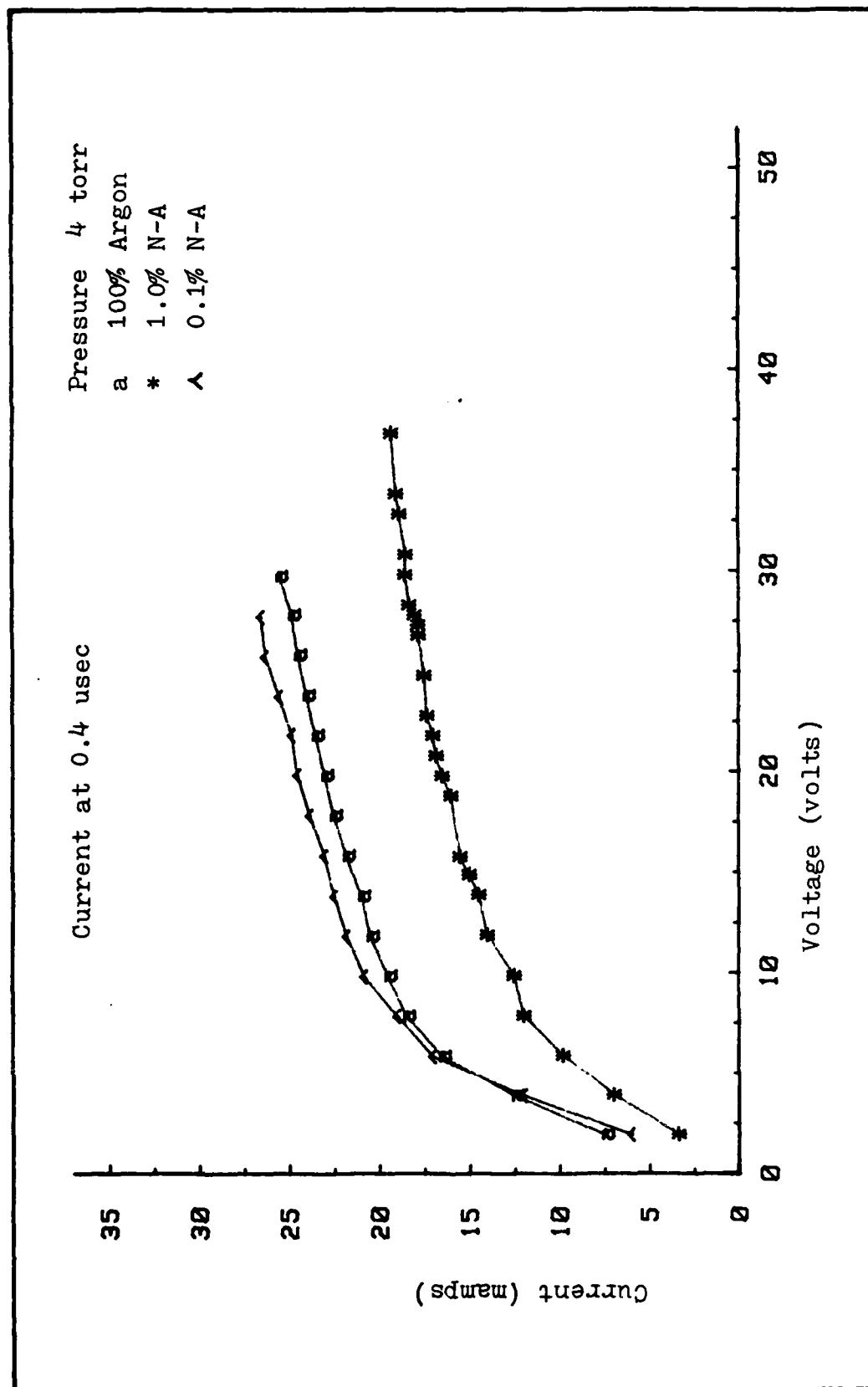


Figure 26. Pulsed I-V Characteristics for Discharge Tube II (4.0 torr)

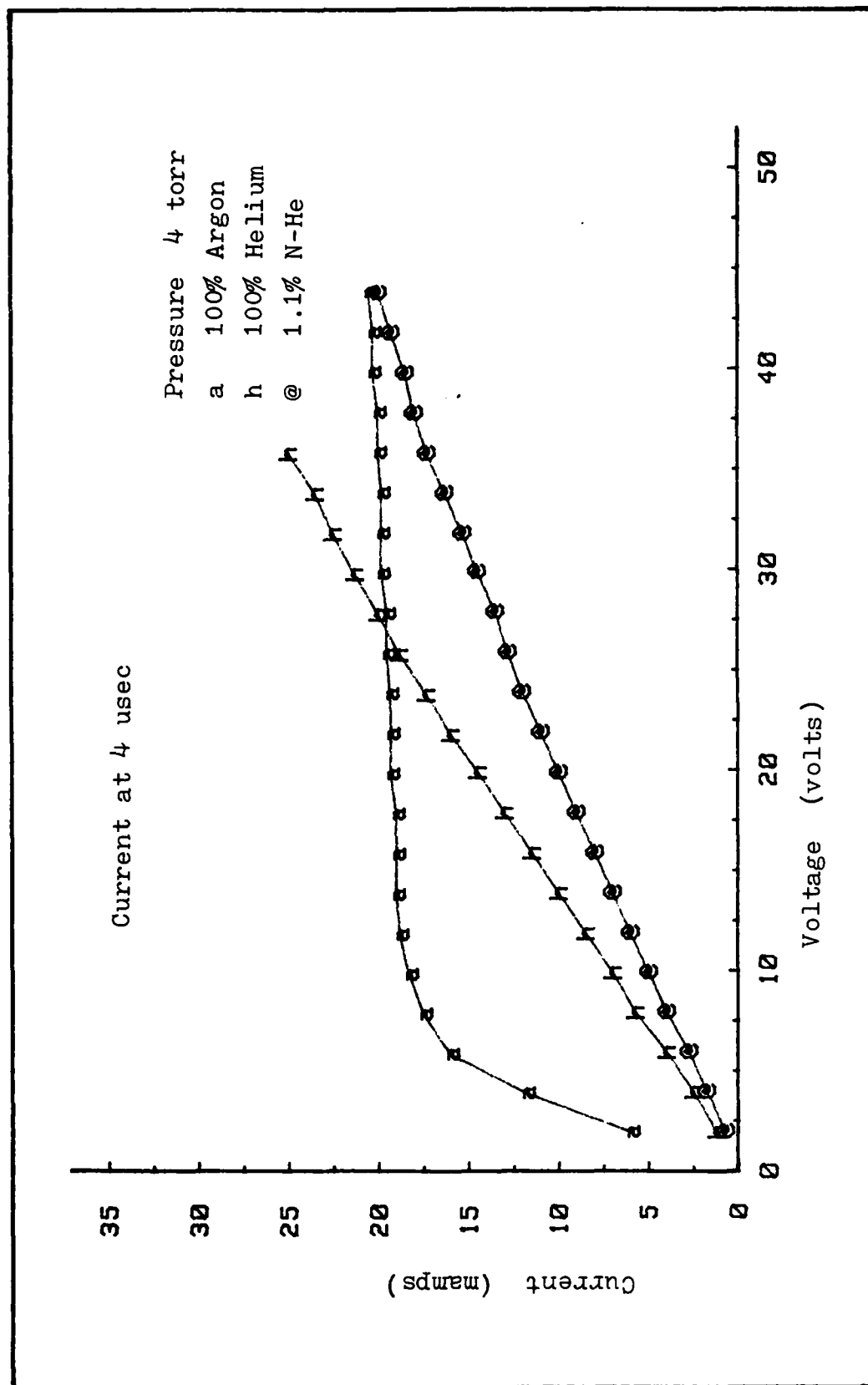


Figure 27. Pulsed I-V Characteristics for Discharge Tube II (4.0 torr)

Vita

Jeremy A. Thorne was born on 16 October 1945 in Detroit, Michigan. He spent six years in the U.S. Army after completion of high school. In December of 1978 he earned a Bachelor of Science degree in Electrical Engineering. He entered the U.S. Air Force in January of 1979 and was commissioned in April of that year. He was assigned to the Advanced Concepts Branch of the Air Force Weapons Laboratory at Kirtland AFB, New Mexico until entering the School of Engineering, Air Force Institute of Technology, in June 1981.

Permanent address: 215 E. Palm Ave., Apt 910
Tampa, Florida 33604

This thesis was typed by Mrs Anna L. Lloyd.

REPORT DOCUMENTATION PAGE		READ INSTRUCTIONS BEFORE COMPLETING FORM
1. REPORT NUMBER AFIT/GEO/PH/82D-14	2. GOVT ACCESSION NO.	3. RECIPIENT'S CATALOG NUMBER
4. TITLE (and Subtitle) DISCHARGE UNDER THE COMBINED INFLUENCE OF DC AND RF FIELDS		5. TYPE OF REPORT & PERIOD COVERED MS Thesis
7. AUTHOR(s) Jeremy A. Thorne 1 Lt		6. PERFORMING ORG. REPORT NUMBER
9. PERFORMING ORGANIZATION NAME AND ADDRESS Air Force Institute of Technology (AFIT-EN) Wright-Patterson Air Force Base, Ohio		8. CONTRACT OR GRANT NUMBER(s)
11. CONTROLLING OFFICE NAME AND ADDRESS AFWAS/POOC-3 Wright-Patterson Air Force Base, Ohio 45433		10. PROGRAM ELEMENT, PROJECT, TASK AREA & WORK UNIT NUMBERS 2301S288
14. MONITORING AGENCY NAME & ADDRESS (if different from Controlling Office)		12. REPORT DATE December 1982
		13. NUMBER OF PAGES 124
		15. SECURITY CLASS. (of this report) Unclassified
		15a. DECLASSIFICATION/DOWNGRADING SCHEDULE
16. DISTRIBUTION STATEMENT (of this Report) Approved for Public release; distribution unlimited		
17. DISTRIBUTION STATEMENT (of the abstract entered in Block 20, if different from Report)		
18. SUPPLEMENTARY NOTES Approved for public release: IAW AFR 190-17. LYNN E. WOLAVER Dean for Research and Professional Development Air Force Institute of Technology (AFIT) Wright-Patterson AFB OH 45433 Approved for public release; IAW AFR 190-17 Fredric C. Lynch, Major, USAF Director, Public Affairs		
19. KEY WORDS (Continue on reverse side if necessary and identify by block number) Microwave Microwave Discharge Cathode Sheath RF Discharge Argon, Argon-Nitrogen		
20. ABSTRACT (Continue on reverse side if necessary and identify by block number) Cold cathode discharges is argon and argon-nitrogen mixtures were investigated experimentally. Current-voltage characteristics were obtained experimentally for these in microwave sustained discharges. The current-voltage characteristics show current saturating at low values of E/N followed by a rapid increase in current at higher E/N. Lowke's theoretical investigation of gas discharges sustained by an external ionizing source was extended to include microwave excitation.		

This analysis predicted a similar saturation for the current in the current-voltage characteristics.

- ¹ J.J. Lowke, D.K. Davies, J. Appl. Phys. 48(12):4991 (1977).

END

FILMED

1-84

DTIC